Supplementary Information (SI) for Physical Chemistry Chemical Physics.

A Comprehensive Statistical Approach to Identify Correct Types of Cross Peaks Based on its Symmetric Feature

Linchen Xie [a, b], Anqi He [b], Limin Yang [c*], Yukihiro Ozaki [b, d],
Isao Noda[b, e], Yizhuang Xu [b*], Kun Huang [a*]

[a] School of Metallurgical and Ecological Engineering, University of Science and Technology Beijing, Beijing 100083, China

[b] Beijing National Laboratory for Molecular Sciences, State Key Laboratory for Rare Earth Materials Chemistry and Applications, College of Chemistry and Molecular Engineering, Peking University, Beijing 100871, China

[c] State Key Laboratory of Nuclear Physics and Technology, Institute of Heavy Ion Physics, School of Physics, Peking University, Beijing 100871, China

[d] School of Biological and Environmental Sciences, Kwansei Gakuin University, Sanda, Hyogo 669-1330, Japan

[e] Department of Materials Science and Engineering, University of Delaware, Newark, Delaware 19716, United States

---

*Corresponding authors: Kun Huang (huangkun@ustb.edu.cn); Limin Yang (yanglm@pku.edu.cn); Yizhuang Xu (xyz@pku.edu.cn)

Table of contents

Part 1 A brief description of the DAOSD approach

DAOSD (double asynchronous orthogonal sample design scheme) is used to reveal subtle spectral variation caused by intermolecular interaction. The description of the DAOSD approach in detail can be found in our previous paper [S1-1]. Here we provide a brief description of the DAOSD approach.

We use the following model system to show how the DAOSD approach works. The model system is: two compounds (denoted as P and Q) are dissolved in the same solutions. Under intermolecular interactions between P and Q, part of P undergoes a subtle structural variation and converts into U. Similarly, part of Q converts into V. The interaction could be described by an equilibrium reaction shown in Eq. S1-1, where K is the equilibrium constant.

$$\mathrm{P}+\mathrm{Q}\overset{K}{\Leftrightarrow}\mathrm{U}+\mathrm{V} \tag{S1-1}$$

In a spectrum of a sample solution, the solvent has no spectral contribution in the spectral region investigated. P has an absorption peak at X_P, and Q has an absorption peak at X_Q. U has an absorption peak at X_U, and V has an absorption peak at X_V. The spectral functions of characteristic peaks of P, Q, U, and V are described by Gaussian functions shown in Eq. S1-2.

$$f_j(x)=\varepsilon_j e^{-(\ln 2)\left[\frac{(x-X_j)^2}{W_j^2}\right]}=\varepsilon_j g_j(x) \tag{S1-2}$$

where j stands for the four chemical species P, Q, U, V; *x* is wavelength;

W_j, X_j, and ε_j are the bandwidth, peak position, and intensity of the characteristic peak of the j^{th} chemical species; $g_j(x)$ is the peak-shape function of the j^{th} chemical species.

Since the structural variation caused by the intermolecular interaction is quite weak, the characteristic peak of U is quite close to that of P. In a similar manner, the characteristic peak of V is quite close to that of Q. In other words, the characteristic peaks of P and U are severely overlapped. Moreover, the characteristic peaks of Q and V are severely overlapped. On the other hand, only a very small fraction of P and Q are converted into U and V since the intermolecular interaction between P and Q is quite weak, Thus, the equilibrium concentrations of P and Q are overwhelmingly larger than those of U and V. Consequently, the characteristic peaks of U and V are buried by the peaks of P and Q. In other words, it is almost impossible to observe any spectral feature of U and V from the original 1D spectra of a sample solution containing P and Q.

To characterize the intermolecular interaction between P and Q, a 2D asynchronous spectrum is generated using the DAOSD approach. In the DAOSD approach, two groups of sample solutions are prepared. Each group contains four sample solutions. In the first group of sample solutions, the initial concentrations of P are constants, while the initial concentrations of Q are selected arbitrarily. In the second group of sample solutions, the initial concentrations of Q are constants, while the initial concentrations of

P are selected arbitrarily. The initial concentrations of P and Q are listed in **Table S1-1**.

Table S1-1 Initial concentrations of P and Q in the model system, which meet the requirement of the DAOSD approach

Index of the solutions	Initial concentrations of P	Initial concentrations of Q
Group 1		
1	10	0
2	10	4
3	10	6
4	10	10
Group 2		
1	0	10
2	4	10
3	6	10
4	10	10

Then, the 1D spectra of the two groups of sample solutions are simulated, and we use the two groups of spectra to construct a pair of 2D asynchronous spectra via Eq. S1-3.

$$\boldsymbol{\Psi} = \mathbf{A}^{T}\mathbf{N}\mathbf{A} \qquad \text{(S1-3)}$$

where **N** is the Hilbert-Noda transformation matrix, and superscript ^{T}

stands for transpose.

The 2D asynchronous spectrum generated via the first group of 1D spectra, where the initial concentrations of P are invariant is denoted as $\boldsymbol{\Psi}_P$. The 2D asynchronous spectrum generated via the second group of 1D spectra, where the initial concentrations of Q are invariant is denoted as $\boldsymbol{\Psi}_Q$.

Results from both the mathematical analysis and computer simulation have proved that:

1) If no intermolecular interaction occurs between P and Q (this can be achieved by setting the value of K in Eq. S1-1 as zero), no cross-peak is produced in either $\boldsymbol{\Psi}_P$ or $\boldsymbol{\Psi}_Q$.

2) If intermolecular interaction indeed occurs between P and Q (this can be accomplished by setting K in Eq. S1-1 as a non-zero value. Herein, the value of K is set as 0.01), cross-peaks may be produced in $\boldsymbol{\Psi}_P$ and $\boldsymbol{\Psi}_Q$.

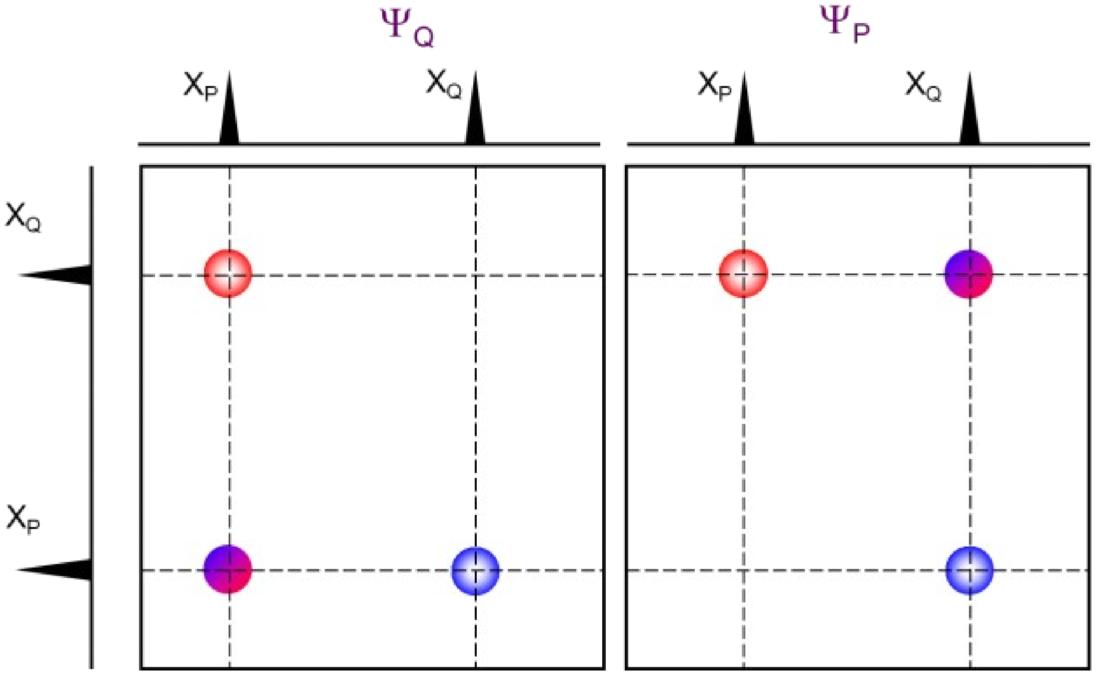

Scheme S1-1 Typical Ψ_P and Ψ_Q.

Scheme S1-1 shows typical Ψ_P and Ψ_Q. In Ψ_P, three groups of cross-peaks appear around (X_P, X_P), (X_P, X_Q), and (X_Q, X_P). In Ψ_Q, three groups of cross-peaks appear around (X_Q, X_Q), (X_P, X_Q), and (X_Q, X_P).

According to the mathematical analysis shown in our previous paper [S1-1], the cross-peak group around (X_Q, X_Q) in Ψ_P reflects the changes of the characteristic peak of Q caused by intermolecular interaction. Furthermore, the spectral function of the cross-peak group can be expressed as Eq. S1-4a. In a similar manner, the cross-peak group around (X_P, X_P) in Ψ_Q reflects the changes of the characteristic peak of P caused by intermolecular interaction. Furthermore, the spectral function of the cross-peak group can be expressed as Eq. S1-4b.

$$\boldsymbol{\Psi}_P(x,y)=\varepsilon_Q\varepsilon_V\left[g_Q(x)g_V(y)-g_Q(y)g_V(x)\right]\left(\vec{\tilde{\mathbf{C}}}_Q^{\text{init}}\right)^T\mathbf{N}\vec{\tilde{\mathbf{C}}}_V^{\text{eq}} \qquad \text{(S1-4a)}$$

$$\mathbf{\Psi}_{Q}(x,y)=\varepsilon_{P}\varepsilon_{U}\left[g_{P}(x)g_{U}(y)-g_{P}(y)g_{U}(x)\right]\left(\vec{\tilde{\mathbf{C}}}_{P}^{init}\right)^{T}\mathbf{N}\vec{\tilde{\mathbf{C}}}_{U}^{eq} \tag{S1-4b}$$

where $\vec{\tilde{\mathbf{C}}}_{P}^{init}$, $\vec{\tilde{\mathbf{C}}}_{U}^{eq}$ are respectively, the initial concentrations of P and the equilibrium concentrations of U in the second group of solutions shown in **Table S1-1**; $\vec{\tilde{\mathbf{C}}}_{Q}^{init}$, $\vec{\tilde{\mathbf{C}}}_{V}^{eq}$ are respectively.

Eq. S1-4a demonstrates that the pattern of cross-peaks around (X_Q, X_Q) in Ψ_P reflects the difference between $g_Q(x)$ and $g_V(x)$. Since $g_Q(x)$ and $g_V(x)$ are relevant to X_Q, X_V, W_Q, and W_V, the pattern of cross-peaks around (X_Q, X_Q) in Ψ_P reflects the changes in peak position and peak width of Q caused by intermolecular interaction.

In a similar manner, Eq. S1-4b demonstrates that the pattern of cross-peaks around (X_P, X_P) in Ψ_Q reflects the difference between $g_P(x)$ and $g_U(x)$. Since $g_P(x)$ and $g_U(x)$ are relevant to X_P, X_U, W_P, and W_U. the pattern of cross-peaks around (X_Q, X_Q) in Ψ_P reflects the changes in peak-position and peak-width of Q caused by intermolecular interaction.

We use the cross-peaks around (X_P, X_P) in Ψ_Q as an example to show the relationship between the patterns of cross-peaks and the variations in peak-position and peak-width. In this case, X_U and W_U are set as variables and we define $\Delta X= X_U - X_P$, $\Delta W= W_U - W_P$. As shown in **Scheme S1-2**, there is a one-to-one correspondence between the pattern of cross-peaks and the combination of ΔX, ΔW.

From a qualitative point of view, the variation of the peak-position and peak-width of U with respect to those of P can be classified into nine situations (**Table S1-2**). The peak parameters of the absorption peak of P are provided in **Table S1-3**. There is a one-to-one correspondence between the patterns of cross-peaks around (X_P, X_P) and the aforementioned nine situations (**Scheme S1-2**).

Table S1-2 The nine classes of the combinations of ΔX and ΔW. The peak parameters for u in the nine classes can be found in **Table S1-3**.

Situation	Peak-position	Peak-width
1	$\Delta X<0$	$\Delta W<0$
2	$\Delta X=0$	$\Delta W<0$
3	$\Delta X>0$	$\Delta W<0$
4	$\Delta X>0$	$\Delta W=0$
5	$\Delta X=0$	$\Delta W=0$
6	$\Delta X<0$	$\Delta W=0$
7	$\Delta X>0$	$\Delta W>0$
8	$\Delta X=0$	$\Delta W>0$
9	$\Delta X<0$	$\Delta W>0$

Table S1-3 Peak parameters of P and U in the model system

	Situation	Peak position	Peak width	Absorptivity
U	1	99	19	1.0
	2	100	19	1.0
	3	101	19	1.0
	4	101	20	1.0
	5	100	20	1.0
	6	99	20	1.0
	7	101	21	1.0
	8	100	21	1.0
	9	99	21	1.0
P		100	20	1.0

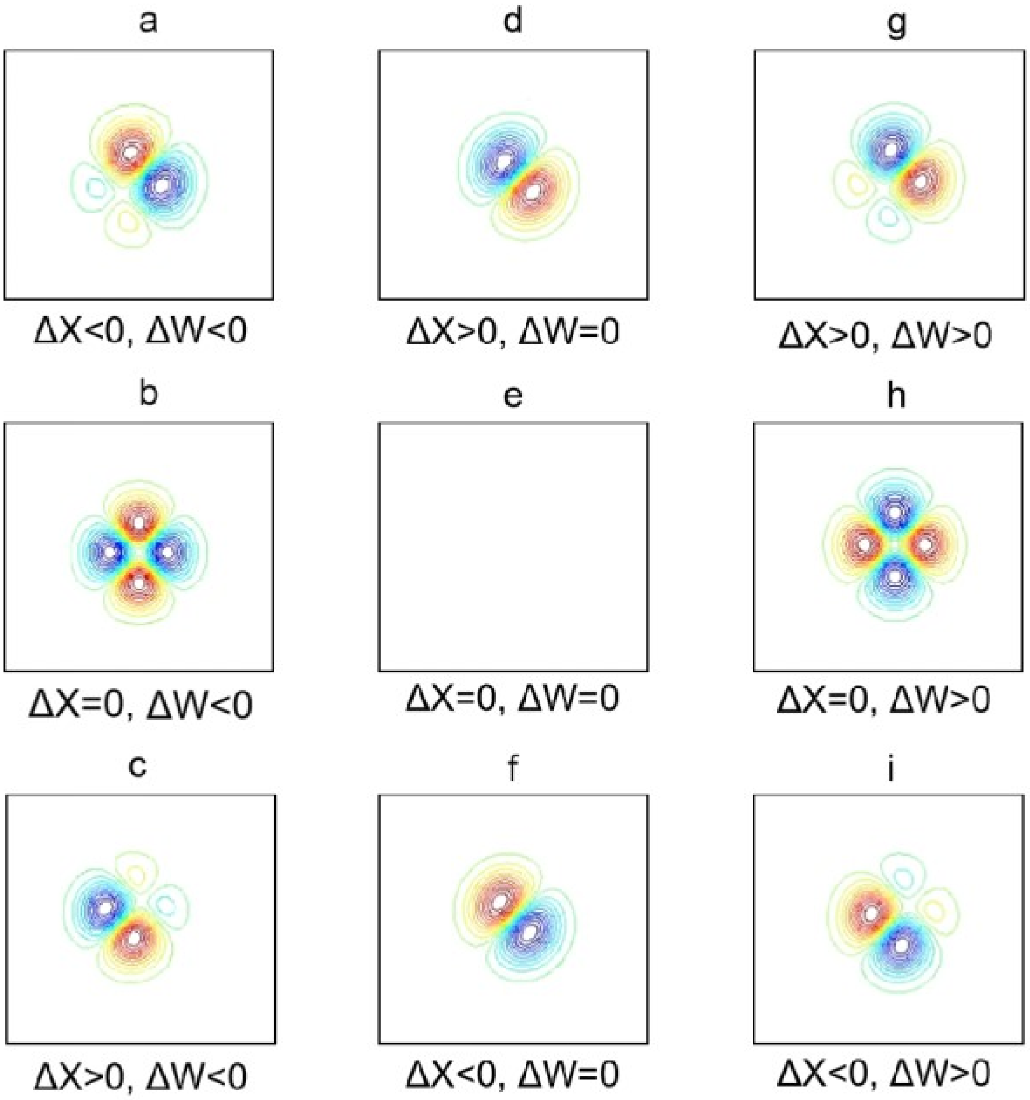

Scheme S1-2. The one-to-one correspondence between the pattern of cross-peaks around (X_P, X_P) in Ψ_Q and the combination of ΔX, ΔW.

From the characteristic pattern of the cross-peak, we can deduce whether the characteristic peak of P undergoes a red shift, or blue shift or remains unchanged under the influence of intermolecular interaction. Moreover, we can also judge whether the peak-width of the peak of P increases, decreases, or remains invariant under the intermolecular interaction. Similar results can also be obtained from the cross-peaks around (X_Q, X_Q) in Ψ_P.

On the other hand, Eq. S1-4a demonstrates that the difference between ε_Q and ε_V can only be reflected by the changes in the intensities of the cross-peak (X_Q, X_Q) in Ψ_P. Similarly, Eq. S1-4b demonstrates that the difference between ε_P and ε_U can only be reflected by the changes in the intensities of the cross-peak (X_P, X_P) in Ψ_Q. In a 2D asynchronous spectrum, the intensities of cross-peaks are affected by multiple factors. Thus, neither the cross-peaks around (X_P, X_P) in Ψ_Q, nor those around (X_P, X_P) in Ψ_Q are suitable to reflect the intensity changes of the characteristic peaks caused by intermolecular interaction.

Then, we come to the group of cross-peaks around (X_P, X_Q) and those around (X_P, X_Q) in Ψ_P. Since the two groups of cross-peaks are antisymmetric with respect to the diagonal, we just discuss the cross-peaks around (X_P, X_Q) in Ψ_P. According to the mathematical analysis in our previous paper [S1-1], the cross-peaks reflect changes in the characteristic peak of P at X_P only. Moreover, the spectral function of the cross-peaks can be expressed as Eq. S1-5.

$$\begin{aligned}\boldsymbol{\Psi}_{\mathrm{P}}(x,y)={}&\varepsilon_{\mathrm{Q}}\varepsilon_{\mathrm{U}}\left[g_{\mathrm{U}}(x)-g_{\mathrm{P}}(x)\right]\left(\vec{\tilde{\mathbf{C}}}_{\mathrm{U}}^{\mathrm{eq}}\right)^{\mathrm{T}}\mathbf{N}\vec{\tilde{\mathbf{C}}}_{\mathrm{Q}}^{\mathrm{init}}\\&+\varepsilon_{\mathrm{Q}}\left(\varepsilon_{\mathrm{U}}-\varepsilon_{\mathrm{P}}\right)g_{\mathrm{P}}(x)g_{\mathrm{Q}}(y)\left(\vec{\tilde{\mathbf{C}}}_{\mathrm{U}}^{\mathrm{eq}}\right)^{\mathrm{T}}\mathbf{N}\vec{\tilde{\mathbf{C}}}_{\mathrm{Q}}^{\mathrm{init}}\end{aligned}\qquad\text{(S1-5)}$$

From Eq. S1-5, the cross-peaks in this region are composed of two parts: the first part ($\varepsilon_{\mathrm{Q}}\varepsilon_{\mathrm{U}}\left[g_{\mathrm{U}}(x)-g_{\mathrm{P}}(x)\right]\left(\vec{\tilde{\mathbf{C}}}_{\mathrm{U}}^{\mathrm{eq}}\right)^{\mathrm{T}}\mathbf{N}\vec{\tilde{\mathbf{C}}}_{\mathrm{Q}}^{\mathrm{init}}$) reflects the variations of bandwidth and peak position of the characteristic peak of P; The nine basic patterns of cross-peaks from the first part ($\varepsilon_{\mathrm{Q}}\varepsilon_{\mathrm{U}}\left[g_{\mathrm{U}}(x)-g_{\mathrm{P}}(x)\right]\left(\vec{\tilde{\mathbf{C}}}_{\mathrm{U}}^{\mathrm{eq}}\right)^{\mathrm{T}}\mathbf{N}\vec{\tilde{\mathbf{C}}}_{\mathrm{Q}}^{\mathrm{init}}$) are illustrated in **Scheme S1-3**.

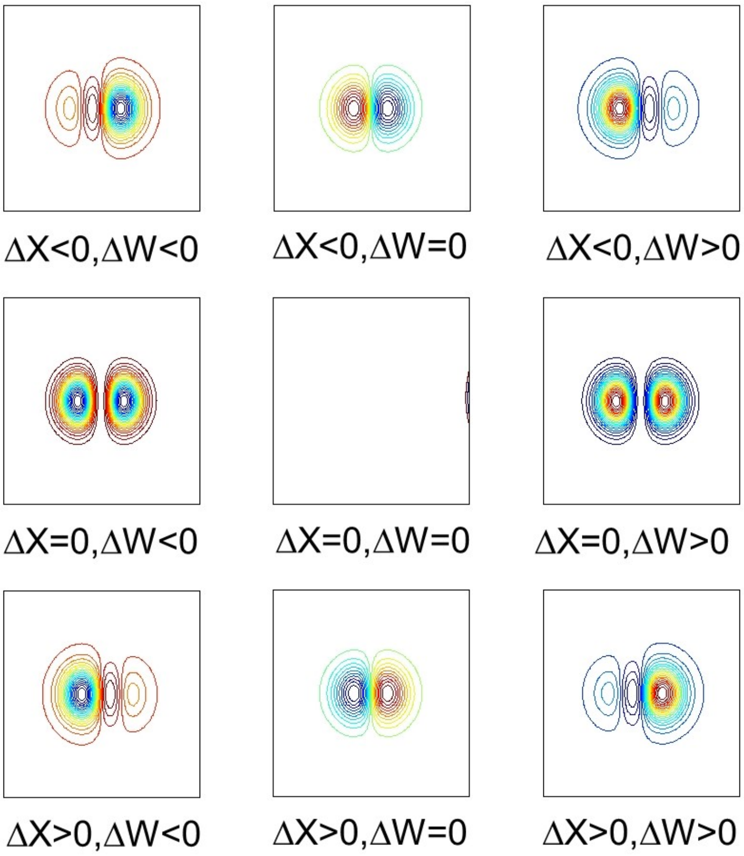

Scheme S1-3 The nine basic patterns of cross-peak around (X_{P}, X_{Q}) derived from $\varepsilon_{\mathrm{Q}}\varepsilon_{\mathrm{U}}\left[g_{\mathrm{U}}(x)-g_{\mathrm{P}}(x)\right]\left(\vec{\tilde{\mathbf{C}}}_{\mathrm{U}}^{\mathrm{eq}}\right)^{\mathrm{T}}\mathbf{N}\vec{\tilde{\mathbf{C}}}_{\mathrm{Q}}^{\mathrm{init}}$ versus the combinations of ΔX, ΔW.

The second part ($\varepsilon_{\mathrm{Q}}\varepsilon_{\mathrm{U}}\left[g_{\mathrm{U}}(x)-g_{\mathrm{P}}(x)\right]\left(\vec{\tilde{\mathbf{C}}}_{\mathrm{U}}^{\mathrm{eq}}\right)^{\mathrm{T}}\mathbf{N}\vec{\tilde{\mathbf{C}}}_{\mathrm{Q}}^{\mathrm{init}}$) reveals the variation of intensity of the characteristic peak of P. Herein, we define $\Delta\varepsilon=\varepsilon_{\mathrm{U}}-\varepsilon_{\mathrm{P}}$. The basic pattern of $\varepsilon_{\mathrm{Q}}\left(\varepsilon_{\mathrm{U}}-\varepsilon_{\mathrm{P}}\right)g_{\mathrm{P}}(x)g_{\mathrm{Q}}(y)\left(\vec{\tilde{\mathbf{C}}}_{\mathrm{U}}^{\mathrm{eq}}\right)^{\mathrm{T}}\mathbf{N}\vec{\tilde{\mathbf{C}}}_{\mathrm{Q}}^{\mathrm{init}}$ is illustrated in **Scheme S1-4**.

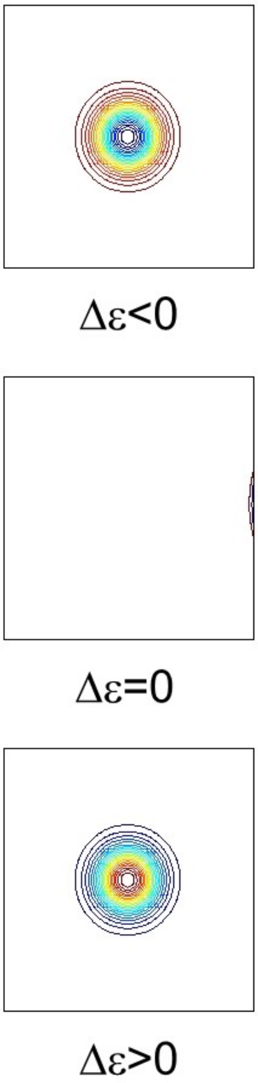

Scheme S1-4 The three basic patterns of cross-peaks derived from $\varepsilon_{Q}(\varepsilon_{U}-\varepsilon_{P})g_{P}(x)g_{Q}(y)\left(\overline{\overline{\mathbf{C}}}_{U}^{eq}\right)^{T}\mathbf{N}\overline{\overline{\mathbf{C}}}_{Q}^{init}$ versus ΔΕ.

The cross-peaks around (X_Q, X_P) in Ψ_Q can be used to reveal the subtle changes of the characteristic peak of Q under the intermolecular interaction via a similar fashion.

We show how to reveal the variation of the characteristic peaks caused by intermolecular interaction via the patterns of cross-peaks from the two 2D asynchronous spectra generated using the DAOSD approach.

The peak parameters for the characteristic peaks of P and Q are listed in **Table S1-4**.

Table S1-4 Peak parameters of P and Q in the model system

j	X_j (nm)	W_j (nm)	ε_j
P	100	20	1.0
Q	300	20	1.0

Since the peaks of U and V overlap with those of P and Q severely. It is impossible to obtain the U, V from the original 1D spectra of the P, Q mixture.

When the DAOSD approach is adopted, Ψ_P and Ψ_Q are obtained and shown in **Figure S1-1A** and **Figure S1-1B**.

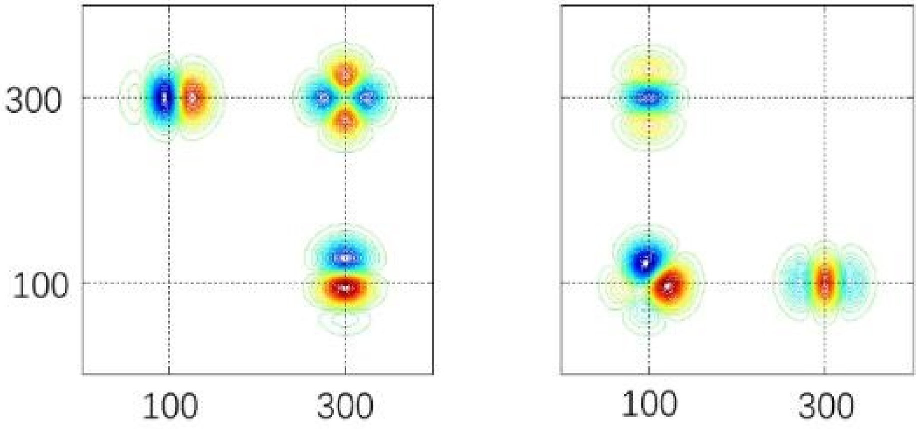

Ψ_P Ψ_Q

A B

Figure S1-1 A Ψ_P; B Ψ_P.

In comparison between the cross-peaks around (300, 300) in Ψ_P and the basic patterns of cross-peak shown in **Scheme S1-2**, the peak position of the characteristic peak of Q remains unchanged, but the peak width decreases under the intermolecular interaction ($\Delta X_Q = 0$, $\Delta W_Q < 0$). Under this situation, the part of cross-peaks around (300, 100) in Ψ_Q, which is relevant to the changes of peak position and peak width is shown in **Figure S1-2A**. The difference between the cross-peak around (300,100) in Ψ_Q and **Figure S1-2A** is a positive cross-peak at (300,100) (**Figure S1-2B**). This result indicates that the intensity of the characteristic peak of Q increases under the intermolecular interaction ($\Delta\varepsilon_Q > 0$).

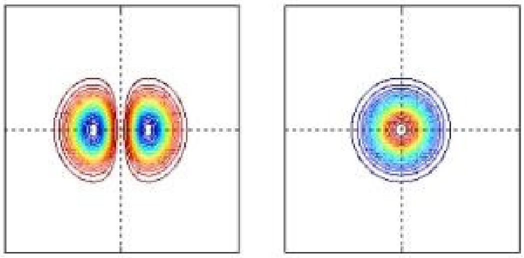

A B

Figure S1-2 A The part of cross-peaks around (300, 100) in Ψ_Q, which is relevant to the changes of peak position and peak width; B The difference between the cross-peak around (300,100) in Ψ_Q and **Figure S1-2A**

Comparison between the cross-peaks around (100, 100) in Ψ_Q and the basic patterns of cross-peak shown in **Scheme S1-3**, both the peak position and the peak width increase under the intermolecular interaction ($\Delta X_P > 0$, $\Delta W_P > 0$).

Under this situation, the part of cross-peaks around (100, 300) in Ψ_P, which is relevant to the changes of peak position and peak width is shown in **Figure S1-3A**. The difference between the cross-peak around (100,300) in Ψ_P and **Figure S1-3A** is a negative cross-peak at (100,300) **(Figure S1-3B**). This result indicates that the intensity of the characteristic peak of P increases under the intermolecular interaction ($\Delta\varepsilon_P < 0$).

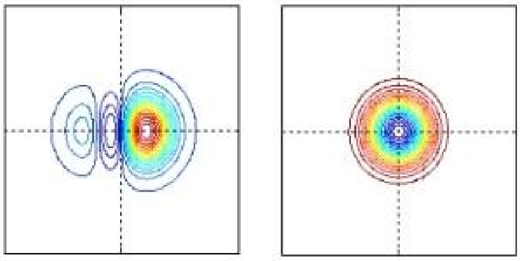

A B

Figure S1-3 A The part of cross-peaks around (100, 300) in Ψ_P, which is relevant to the changes of peak position and peak width; **B** The difference between the cross-peak around (100, 300) in Ψ_P and **Figure S1-3A.** The preset peak parameters of U and V are listed in **Table S1-5**.

Table S1-5 The preset peak parameters of U and V in the model system

j	X_j (nm)	W_j (nm)	ε_j
U	101	21	0.95
V	300	19	1.05

We confirm subtle changes in peak position, peak width, and intensity can be correctly obtained via the characteristic patterns of cross-peaks of the 2D asynchronous spectra generated via the DAOSD approach.

Then, we consider a chemical system containing P, Q. If P has a characteristic peak at X_P, but Q has no spectral contribution in the spectral region investigated. Subtle changes in peak position and peak width can be revealed by the characteristic pattern of cross-peaks around (X_P, X_P) in the 2D asynchronous spectrum. The variation in the intensity of the peak can be deduced by the ASAP approach described in another paper of our previous work [S1-2].

References

S1-1 J. Chen, Q. Bi, S.X. Liu, X. P. Li, Y. H. Liu, Y. J. Zhai, Y. Zhao, L.M. Yang, Y.Z. Xu, I. Noda, J.G. Wu, J. Phys. Chem. A., 2012, **116**, 10904–10916.

S1-2 X.P. Li, A.Q. He, K. Huang, H.Z. Liu, Y. Zhao, Y.J. Wei, Y.Z. Xu, I. Noda, J.G. Wu, Rsc. Adv., 2015, **5**, 87739-87749.

Part 2 Description of the model system 1

In this model system, we try to characterize the intermolecular interaction between two solutes (P and Q) dissolved in the same solutions.

Under the intermolecular interaction between P and Q, part of P and part of Q form a supramolecular aggregate (PQ). The interconversion can be described by a reaction shown in Eq. S2-1.

$$P + Q \overset{K}{\leftrightarrow} PQ \tag{S2-1}$$

where K is the equilibrium constant, and the value of K is set as 0.01 L/mol.

In a spectrum of a sample solution containing P and Q, neither solvent nor Q has any contribution in the spectral region investigated. P has a characteristic peak, and PQ has a characteristic peak.

The characteristic peak of P can be described by a Gaussian function (Eq. S2-2).

$$f_P(x) = \varepsilon_P e^{-(ln2)\left[\frac{(x-X_P)^2}{W_P^2}\right]} = \varepsilon_P g_P(x) \tag{S2-3}$$

where ε_P, X_P, and W_P, respectively are the molar absorptive, peak position, and half-width at the half-height of the characteristic peak of P.

The characteristic peak of PQ can also be described by a Gaussian function (Eq. S2-3).

$$f_{PQ}(x) = \varepsilon_{PQ} e^{-(ln2)\left[\frac{(x-X_{PQ})^2}{W_{PQ}^2}\right]} = \varepsilon_{PQ} g_{PQ}(x) \qquad \text{(S2-3)}$$

where ε_{PQ}, X_{PQ}, and W_{PQ}, respectively are the molar absorptivity, peak position, and half-width at the half-height of the characteristic peak of PQ.

The values of ε_P, X_P, W_P, ε_{PQ}, X_{PQ}, and W_{PQ} are listed in **Table S2-1**.

Table S2-1 Peak parameters of P and PQ in the first model system.

	Peak-position	Bandwidth	Absorptivity
P	305.7	35	1.0
PQ	304.1	35	1.0

To characterize the intermolecular interaction, five 1D spectra of the simulated solutions containing different amount of P and Q are simulated. The initial concentration of P and Q in the five simulated solutions are listed in **Table S2-2**. The simulated 1D spectrum are used to construct a 2D asynchronous spectrum.

Table S2-2 The initial concentrations of P and Q in the five 1D spectra used to construct the 2D asynchronous spectrum

	C_P (mol/L)	C_Q (mol/L)

1	0	0.1
2	0.35	0.1
3	0.37	0.1
4	0.39	0.1
5	0.38	0.1

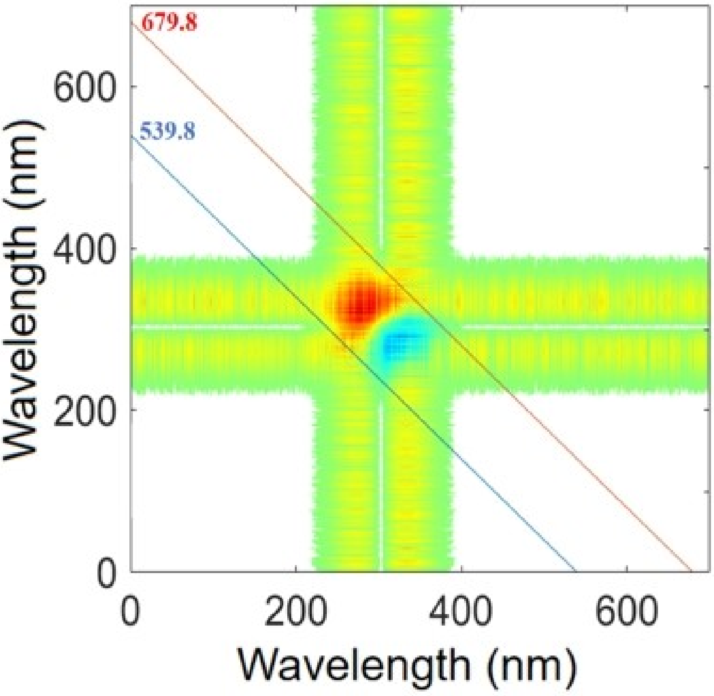

Figure S2-1. The possible range of b in the model system 1.

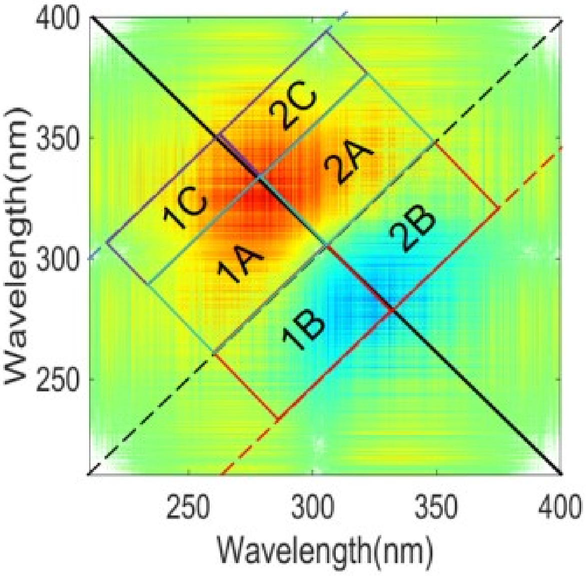

Figure S2-2 Ranges of Ω_{2A}, Ω_{2B}, Ω_{1A} and Ω_{1B}.

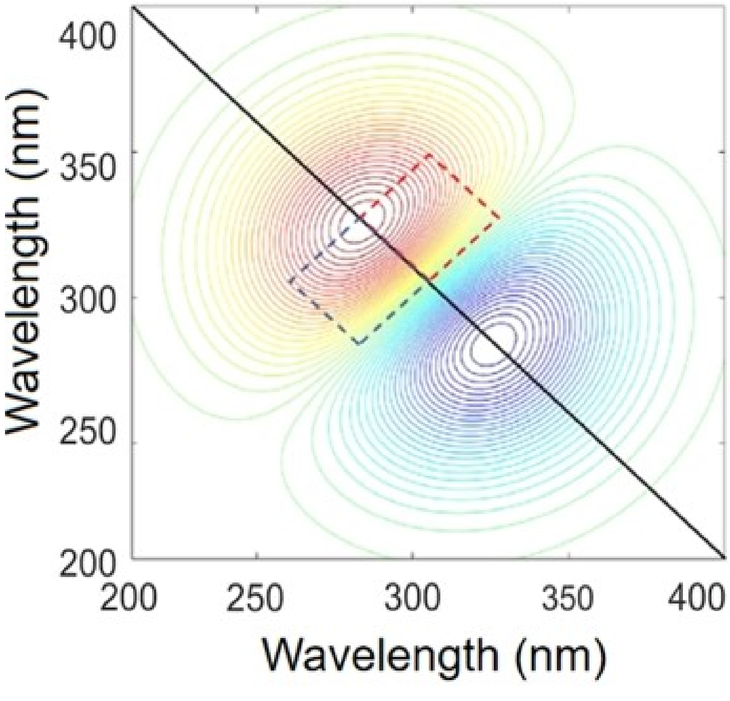

Figure S2-3. The borders of the two rectangular regions (Ω_1 and Ω_2) in the model system 1.

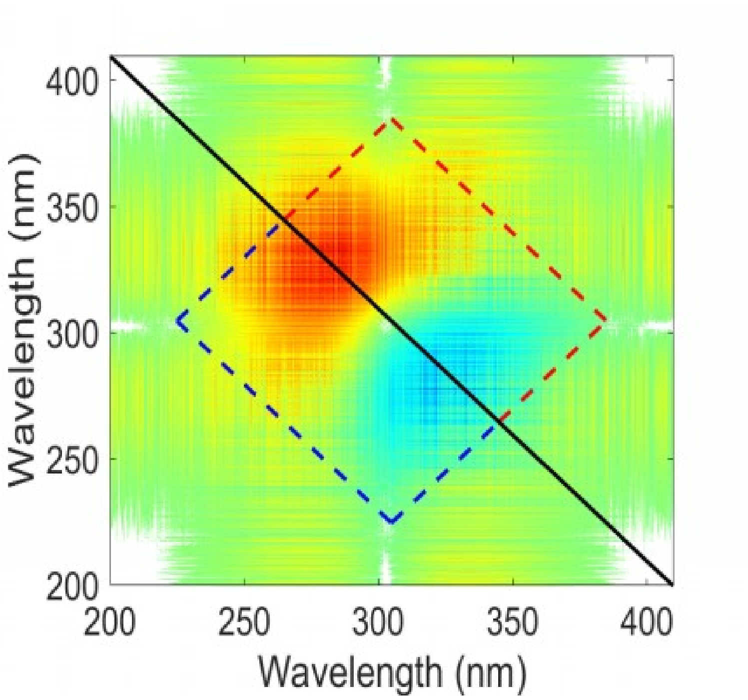

Figure S2-4. Ω_A and Ω_B of the 2D asynchronous spectrum of the model system 1 (the 2D asynchronous spectrum is covered by heavy noise).

The border of Ω_A and Ω_B are straight lines whose function are:

Ω_A: $y = -x + 609.8$; $y =-x + 678.8$; $y = x +90$; $y = x -90$.

Ω_B: $y = -x + 609.8$; $y = -x + 540.8$; $y = x +90$; $y = x -90$.

The random range selection rules:

In the cross-peaks investigated, we supposed mirror symmetry is present, and the equation of the mirror is: $y = -x + \mathrm{b}$, where the method to determine the value of b has been described in the manuscript. For each i, where i {1, 2, …, 15}, ${}^{i}\ {}_{A}$ and ${}^{i}\ {}_{B}$ are mirror symmetric to each other with respect of the mirror ($y = -x + \mathrm{b}$). The shape of ${}^{i}\ {}_{A}$ and

${}^{i}\quad{}_{B}$ are rectangles. The borders of ${}^{i}\quad{}_{A}$ and ${}^{i}\quad{}_{B}$ are defined as below:

${}^{i}\quad{}_{A}$:

$y = -x + b_0$;

$y = -x + {}^{i}b_1$;

$y = x + {}^{i}b_2$;

$y = x + {}^{i}b_3$

${}^{i}\quad{}_{B}$:

$y = -x + b$;

$y = -x + 2b - {}^{i}b_1$;

$y = x + {}^{i}b_2$;

$y = x + {}^{i}b_3$

The value of ${}^{i}b_1$, ${}^{i}b_2$, and ${}^{i}b_3$ are generated randomly.

Since ${}^{i}\quad{}_{A}$ and ${}^{i}\quad{}_{B}$ must be within the cross-peaks group investigated, the values of ${}^{i}b_1$, ${}^{i}b_2$, and ${}^{i}b_3$ are generated within the following regions.

${}^{i}b_1 \in (640, 680)$;

${}^{i}b_2 \in (-90, -6)$;

${}^{i}b_3 \in (90, 6)$

Table S2-3 The values of b_0 ${}^{i}b_1$, ${}^{i}b_2$, and ${}^{i}b_3$ for the 15 2D sub spectral regions selected in a random manner

i	b_0	$^{i}b_1$	$^{i}b_2$	$^{i}b_3$
1	582.8	636.8	-90	90
2	579.8	639.8	-84	84
3	576.8	642.8	-78	78
4	573.8	645.8	-72	72
5	570.8	648.8	-66	66
6	567.8	651.8	-60	60
7	564.8	654.8	-54	54
8	561.8	657.8	-48	48
9	558.8	660.8	-42	42
10	555.8	663.8	-36	36
11	552.8	666.8	-30	30
12	549.8	669.8	-24	24
13	546.8	672.8	-18	18
14	543.8	675.8	-12	12
15	540.8	678.8	-6	6

```
// Pseudo-algorithm: testing the symmetry of 15 sets of data
// input data
data_groups = [group1, group2, ..., group15]
p_values = []
// Perform a K-S test on each set of data
```

```
for each group in data_groups:
    p_value = kolmogorov_smirnov_test(group, mirrored_group)
    p_values.append(p_value)
// Check that all p-values are ≥ 0.05
all_p_above_threshold = True
for p in p_values:
    if p < 0.05:
        all_p_above_threshold = False
        break
// Selection of subsequent steps based on results
if all_p_above_threshold:
    // Performing Bayesian analyses
    symmetry_probability = bayesian_analysis(data_groups)
    output "The probability that symmetry exists is " + symmetry_probability
else:
    output "No symmetry within the cross peaks"
```

Part 3 The mathematical proof of the theorem

Proof: $f_P(x)$ and $f_{PQ}(x)$ can be expressed as Eq. S3-1a and Eq. S3-1b

$$f_P(x)=\varepsilon_P g_P(x) \qquad \text{S3-1a}$$

$$f_{PQ}(x)=\varepsilon_{PQ} g_{PQ}(x) \qquad \text{S3-1b}$$

where ε_P and ε_{PQ} are the absorptivity of the characteristic peaks of P and PQ, respectively; $g_P(x)$ and $g_{PQ}(x)$ are the peak shape functions of the characteristic peaks of P and PQ.

Since the shapes' spectral function of P and that of PQ are the same, we have:

$$g_{PQ}(x)= g_P(x\text{-}2\Delta) \qquad \text{S3-2}$$

According to Eq. S1-4b in part 1 of **Supporting Information**, we have

$$\boldsymbol{\Psi}(x, y) = \alpha[g_P(x)g_{PQ}(y)\text{-}\ g_P(y)g_{PQ}(x)] \qquad \text{S3-3}$$

where $\alpha=\varepsilon_P\varepsilon_Q(\vec{\tilde{\mathbf{C}}}_P^{\text{init}})^T\mathbf{N}(\vec{\tilde{\mathbf{C}}}_{PQ}^{\text{eq}})$.

Then, a coordinate translation transformation is performed on the 2D asynchronous spectrum, and the new origin is (δ, δ). The new coordinates are ${}^t x$ and ${}^t y$.

Thus, we have

$${}^t x = x\ \text{-}\delta \qquad \text{S3-4a}$$

$${}^t y = y\ \text{-}\delta \qquad \text{S3-4b}$$

After the coordinate translation transformation, we have the following changes: $x\to{}^t x$; $y\to{}^t y$; $g_P(x) \to {}^t g_P({}^t x)$; $g_{PQ}(x) \to {}^t g_{PQ}({}^t x)$; $\boldsymbol{\Psi}(x, y) \to {}^t\boldsymbol{\Psi}({}^t x,$

${}^{t}y$).

Under the new coordinate system, the values of α remain unchanged. As a result, ${}^{t}\Psi({}^{t}x, {}^{t}y)$ can be expressed as

$$ {}^{t}\boldsymbol{\Psi}({}^{t}x, {}^{t}y) = \alpha[{}^{t}g_{P}({}^{t}x){}^{t}g_{PQ}({}^{t}y) - {}^{t}g_{P}({}^{t}y){}^{t}g_{PQ}({}^{t}x)] \tag{S3-5} $$

Under the new coordinates, the peak positions of P and PQ become -Δ and Δ, respectively. Thus, ${}^{t}g_{P}({}^{t}x)$ is symmetric with respect to ${}^{t}x = -\Delta$; and ${}^{t}g_{PQ}({}^{t}x)$ is symmetric with respect to ${}^{t}x = \Delta$. That is

$$ {}^{t}g_{P}(-\Delta - {}^{t}x) = {}^{t}g_{P}(-\Delta + {}^{t}x) \tag{S3-6a} $$

$$ {}^{t}g_{PQ}(\Delta - {}^{t}x) = {}^{t}g_{PQ}(\Delta + {}^{t}x) \tag{S3-6b} $$

Additionally, the line ($y = -x - 2\delta$) in the old coordinate system has been changed to ${}^{t}y = -{}^{t}x$ in the new coordinate system.

Since the shape of ${}^{t}g_{P}({}^{t}x)$ and ${}^{t}g_{PQ}({}^{t}x)$ are the same, for any given ${}^{t}x_{a}$, we have (**Figure S3-1**)

$$ {}^{t}g_{P}({}^{t}x_{a}) = {}^{t}g_{PQ}({}^{t}x_{a} - 2\Delta) \tag{S3-7} $$

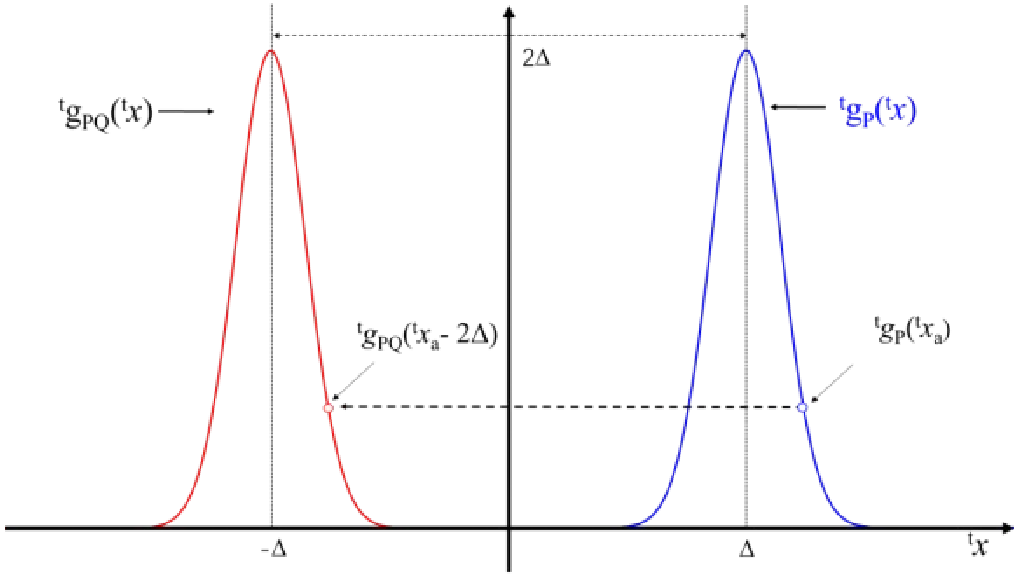

Figure S3-1 The relationship between ${}^{t}g_{P}({}^{t}x_{a})$ and ${}^{t}g_{PQ}({}^{t}x_{a} - 2\Delta)$

For any given ${}^{t}x_a$, we have d_0. The relationship between ${}^{t}x_a$ and d_0 can be expressed as Eq. S3-8 (**Figure S3-2**).

$$ {}^{t}x_a = \Delta + d_0 \tag{S3-8} $$

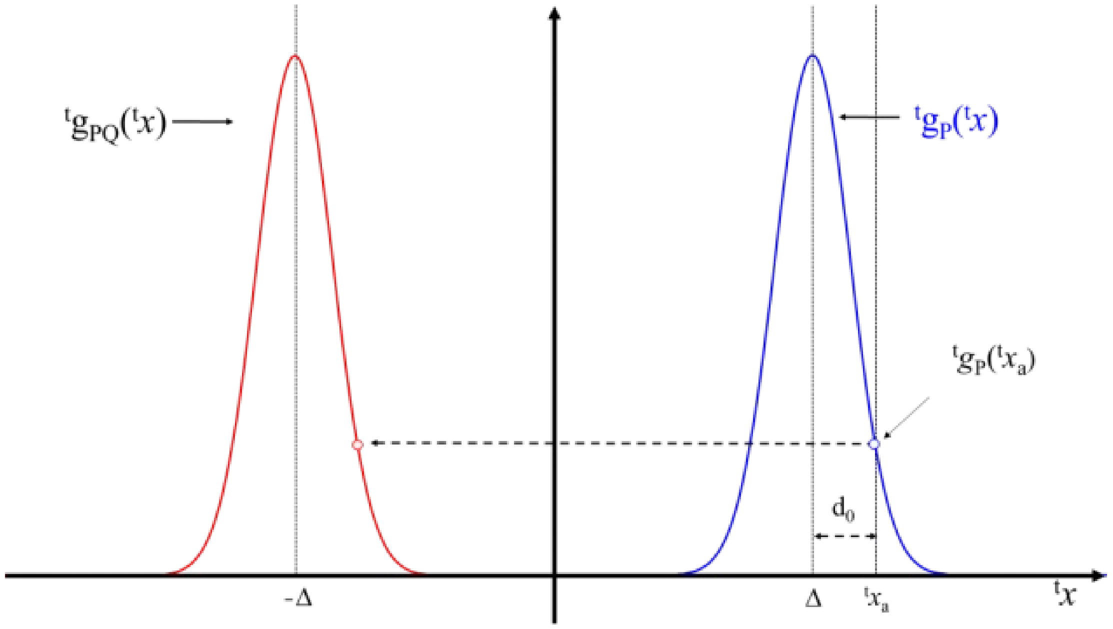

Figure S3-2 The relationship between ${}^{t}x_a$ and $\Delta + d_0$

Thus, we have

$$ {}^{t}g_{PQ}({}^{t}x_a - 2\Delta) = {}^{t}g_{PQ}(-\Delta + d_0) \tag{S3-9} $$

We notice that ${}^{t}g_{PQ}({}^{t}x)$ is symmetric with respect to ${}^{t}x = -\Delta$. As shown in **Figure S3-3**, we have

$$ {}^{t}g_{PQ}(-\Delta + d_0) = {}^{t}g_{PQ}(-\Delta - d_0) \tag{S3-10} $$

According to Eq. S3-8, we have

$$ -\Delta - d_0 = -(\Delta + d_0) = -{}^{t}x_a \tag{S3-11} $$

Thus, Eq. S3-10 can be expressed as

$$ {}^{t}g_{PQ}(-\Delta - d_0) = {}^{t}g_{PQ}(-{}^{t}x_a) \tag{S3-12} $$

After combining Eq. S3-7 to Eq. S3-12, we have

$$ {}^{t}g_{P}({}^{t}x_{a}) = {}^{t}g_{PQ}(-{}^{t}x_{a}) \qquad \text{S3-13} $$

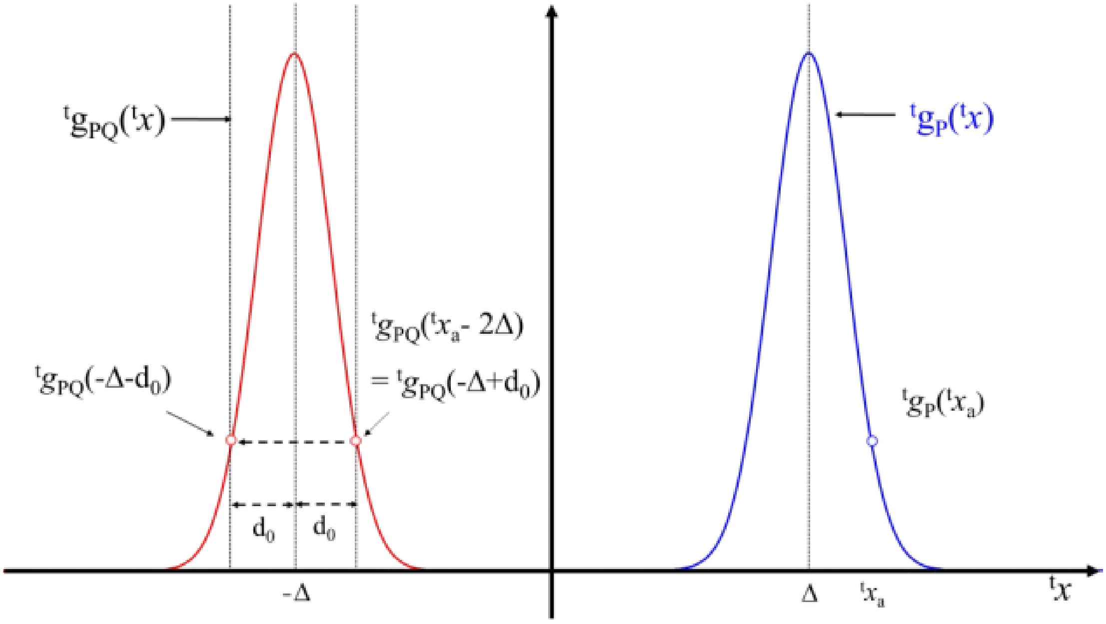

Figure S3-3 The relationship between ${}^{t}g_{PQ}(-\Delta + d_0)$ and ${}^{t}g_{PQ}(-\Delta - d_0)$

Since the shape of ${}^{t}g_{P}({}^{t}x)$ and ${}^{t}g_{PQ}({}^{t}x)$ are the same, for any given ${}^{t}x_{b}$, Eq. S3-14 is true (**Figure S3-4**)

$$ {}^{t}g_{PQ}({}^{t}x_{b}) = {}^{t}g_{P}({}^{t}x_{b} + 2\Delta) \qquad \text{S3-14} $$

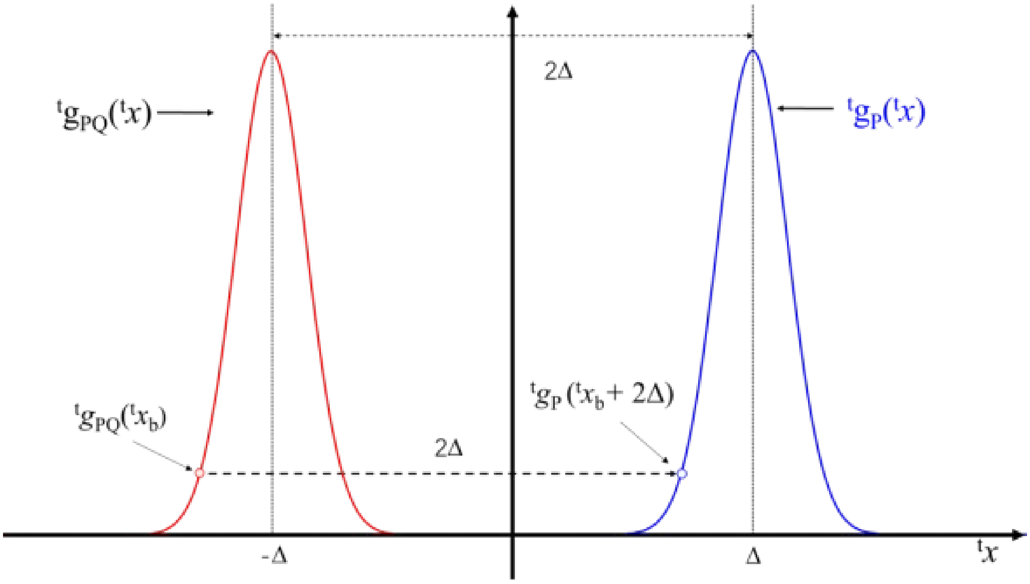

Figure S3-4 The relationship between ${}^{t}g_{PQ}({}^{t}x_{b})$ and ${}^{t}g_{P}({}^{t}x_{b}+2\Delta)$

As shown in **Figure S3-5**, we have

$$ {}^tx_b = -\Delta - d_1 \tag{S3-15} $$

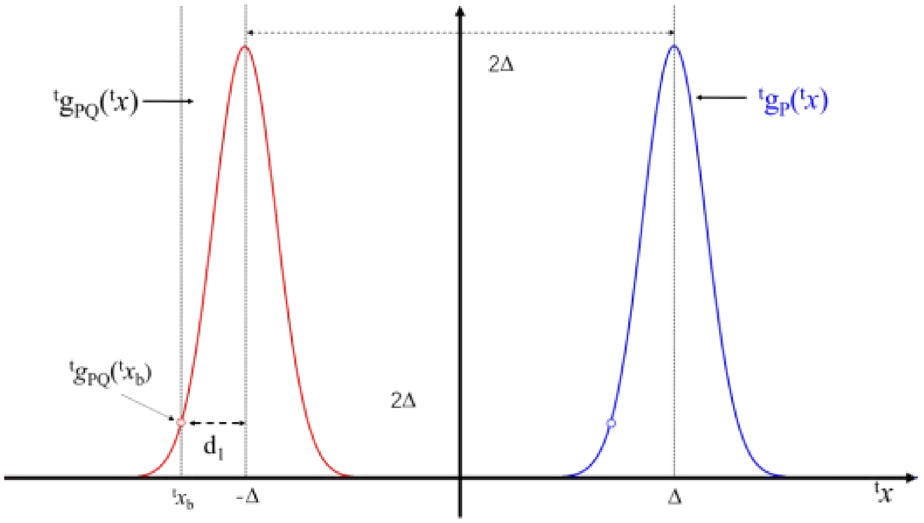

Figure S3-5 The relationship between ${}^tx_b$ and $-\Delta - d_1$

Thus, ${}^tg_P({}^tx_b+2\Delta)$ can be modified as Eq. S3-16.

$$ {}^tg_P({}^tx_b + 2\Delta) = {}^tg_P(\Delta - d_1) \tag{S3-16} $$

Since ${}^tg_P({}^tx)$ is symmetric with respect to ${}^tx = \Delta$ (**Figure S3-6**), we have

$$ {}^tg_P(\Delta - d_1) = {}^tg_P(\Delta + d_1) \tag{S3-17} $$

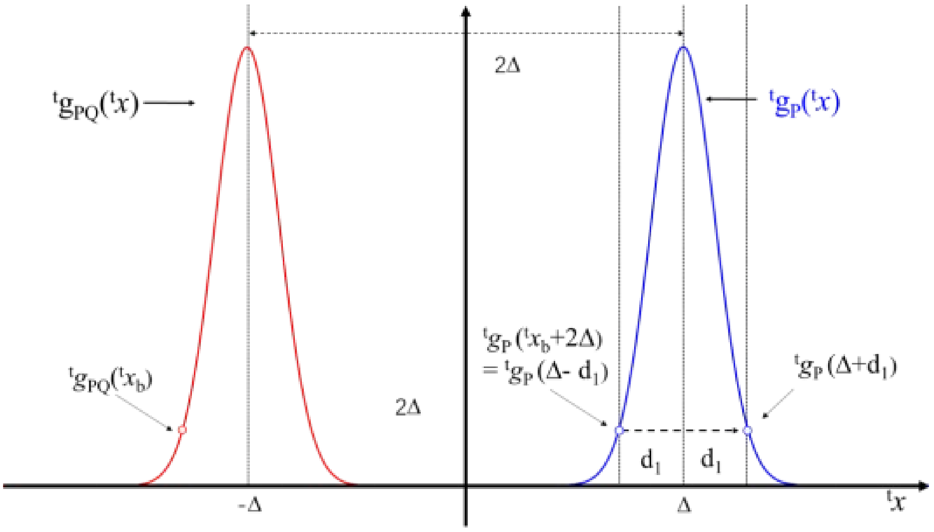

Figure S3-6 The relationship between ${}^tg_P(\Delta - d_1)$ and ${}^tg_P(\Delta + d_1)$

According to Eq. S3-15, we have

$$\Delta + d_1 = -{}^{t}x_b \qquad \text{S3-18}$$

After combining Eq. S3-14 to Eq. S3-18, we have

$${}^{t}g_{PQ}({}^{t}x_b) = {}^{t}g_P(-{}^{t}x_b) \qquad \text{S3-19}$$

When Eq. S3-13 and Eq. S3-19 are incorporated with Eq. S3-5, we have

$$\begin{aligned}
{}^{t}\Psi({}^{t}x, {}^{t}y) &= \alpha[{}^{t}g_P({}^{t}x){}^{t}g_{PQ}({}^{t}y) - {}^{t}g_P({}^{t}y){}^{t}g_{PQ}({}^{t}x)] \\
&= \alpha[{}^{t}g_{PQ}(-{}^{t}x)\,{}^{t}g_P(-{}^{t}y) - {}^{t}g_{PQ}(-{}^{t}y)\,{}^{t}g_P(-{}^{t}x)] \\
&= \alpha[{}^{t}g_P(-{}^{t}y)\,{}^{t}g_{PQ}(-{}^{t}x) - {}^{t}g_P(-{}^{t}x)\,{}^{t}g_{PQ}(-{}^{t}y)] \\
&= {}^{t}\Psi(-{}^{t}y, -{}^{t}x)
\end{aligned} \qquad \text{S3-20}$$

From Eq. S3-20, we learn that ${}^{t}\Psi({}^{t}x, {}^{t}y)$ is symmetric with respect to the line ${}^{t}y = -{}^{t}x$ in the new coordinate system. In the original coordinate, $\Psi(x, y)$ should be symmetric with respect to the line $y = -x - 2\delta$.

The end of the proof.

Part 4 A description of K-S text

In this paper, the Kolmogorov-Smirnov two-sample test (denoted as K-S test hereafter) is used to verify whether the two sets of data come from the same distribution. This part provides a brief description of the Kolmogorov-Smirnov test, and a detailed description of the Kolmogorov-Smirnov test can be found in the literature [S4-1].

In the K-S test, the null hypothesis H_0 and the alternative hypothesis H_1 are defined as follows:

1) H_0 corresponds to the case where there is no significant difference between the two sets of data.

2) H_1 corresponds to the case where there is a significant difference between the two sets of data.

The criterion value α to reject the null hypothesis was set at 0.05.

Herein, we use the following two sets of data (X, Y) as an example to show how to use the K-S test to check whether the two sets of data come from the same distribution.

X = [2.91, -0.93, 1.17, 1.51, 0.5, 2.15, -0.94, -0.65, -0.8, -0.18, 0.23, -1.79, 0.98, -0.22, 0.17, -1.61, -0.65, -0.76, -0.04, -0.21, -1.54, 1.15, -0.5, 1.07, -0.96, 0.45, -1.38, -0.12, -0.57, -1.8, -0.89, -0.2, 0.97, 0.21, -0.61, 0.4, 0.2, 2, -0.31, -2.42, 0.81, 0.77, 1.75, -1.71, -1.26, 1.54, -0.9, 0.27, 0.57, 0.23];

Y = [0.81, -0.29, -0.46, 0.35, -0.86, -0.98, -1, 1.99, -1.23, 0.8, -0.26, 1.13, 0.47, 0, -1.2, 0.35, -2.02, 0.46, -0.17, -1.13, 0.18, 0.53, -0.02, 0.81, 1.22, -

0.73, 1.59, -1.38, 0.94, 0.17, -0.33, 0.3, -0.68, -0.59, -1.53, 0.81, -1.01, -0.73, 0.05, -1.98, -2.2, 0.58, 1.26, 0.09, -0.47, -0.8, -0.12, 0.48, -0.59, -2.5, -0.74].

In this case, the sizes of both X and Y, which are respectively, denoted as m_X and m_Y, are 51.

The analysis is carried out via the following procedure:

1) Both X and Y are rearranged in ascending order. The sorted X and Y are denoted as X_1 and Y_1.

2) Empirical distribution functions for X and Y (denoted as $F_X(t)$, $F_Y(t)$, respectively), were obtained via Eq. S4-1A and Eq. S4-1B.

$$F_X(t) = \begin{cases} 0 & t < X_1(1) \\ \dfrac{j}{m_X} & X_1(j) \le t < X_1(j+1), 1 \le j < m_X \\ 1 & t \ge X_1(m_X) \end{cases} \tag{S4-1A}$$

$$F_Y(t) = \begin{cases} 0 & t < Y_1(1) \\ \dfrac{j}{m_Y} & Y_1(j) \le t < Y_1(j+1), 1 \le j < m_Y \\ 1 & t \ge Y_1(m_X) \end{cases} \tag{S4-1B}$$

3) The value of D_{XY} is calculated via Eq. S4-2. In this case, the value of D_{XY} turns out to be 0.118.

$$D_{XY} = \max\left[F_X(t) - F_Y(t)\right] \tag{S4-2}$$

4) Under the following conditions: 1) $m_X > 50$ or $m_Y > 50$; 2) The criterion value α is set as 0.05, the corresponding c_α, is calculated via Eq. S4-3. The value of c_α is 0.269.

$$c_{\alpha} = 1.36\sqrt{\frac{m_X + m_Y}{m_X m_Y}} = 0.269 \qquad \text{(S4-3)}$$

5) The value of Asymp. Sig., which means asymptotic significance (denoted as P), can be calculated via Eq. S4-4.

$$P = 2e^{-\frac{2}{(1.36)^2}\left(\frac{D_{XY}}{c_{\alpha}}\right)^2} \qquad \text{(S4-4)}$$

If $P \geq 0.05$, we accept the null hypothesis (H_0);

If $P < 0.05$, we reject the null hypothesis (H_0) and accept the alternative hypothesis (H_1).

For the data set X, Y, we have $P = 0.981 > 0.05$, hence, X and Y come from the same distribution.

A brief process of the K-S test is shown in **Scheme S4-1**.

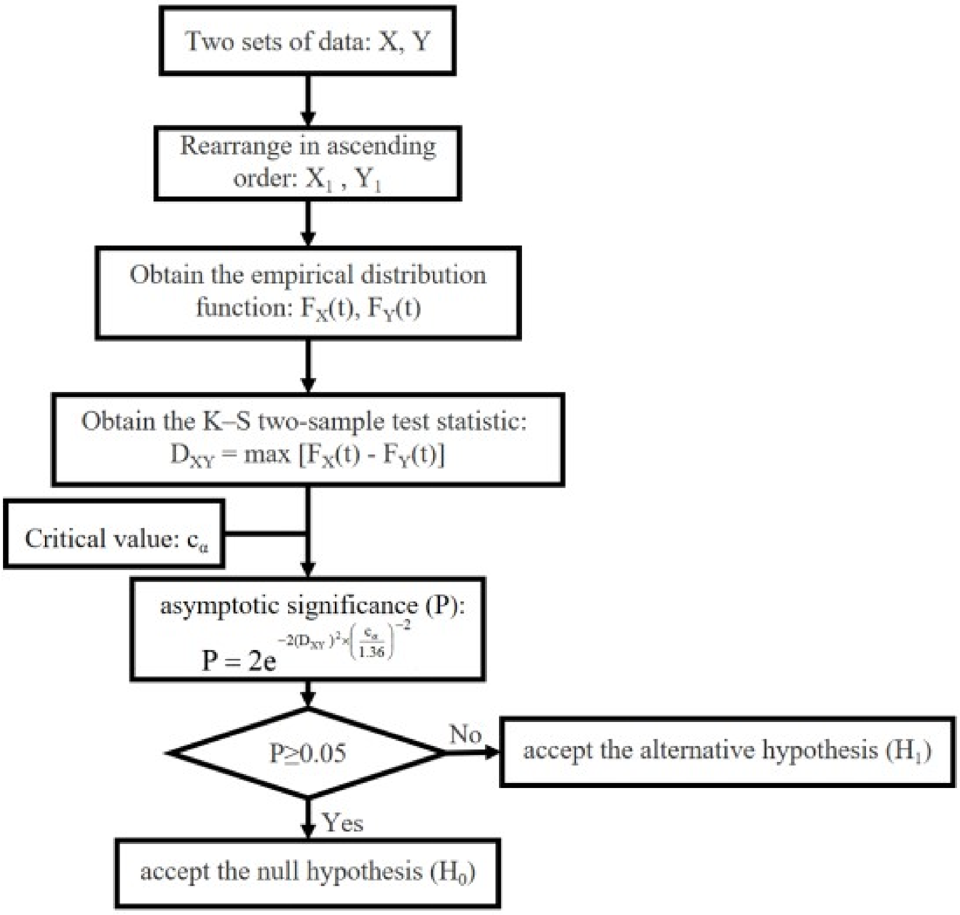

Scheme S4-1 Process of the K-S test.

References

S4-1 J.W. Pratt, J.D. Gibbons, Kolmogorov-Smirnov Two-Sample Tests. Concepts of Nonparametric Theory, 1981, 318–344.

Part 5 The results of the K-S tests in the model system 1

Table S5-1. The P values of the 15 K-S tests in the model system 1.

number	P_i value
1	0.9915
2	0.9462
3	0.9421
4	0.5126
5	0.9682
6	0.9999
7	0.9509
8	0.9474
9	0.4024
10	0.9984
11	0.9996
12	0.0993
13	0.1598
14	0.9999
15	0.8373

Part 6 Description of the model system 2

In this model system, we try to characterize the intermolecular interaction between two solutes (U and V) dissolved in the same solutions.

Under the intermolecular interaction between U and V, part of U and part of V form a supramolecular aggregate (UV). The interconversion can be described by a reaction shown in Eq. S6-1.

$$\mathrm{U} + \mathrm{V} \overset{\mathrm{K}}{\leftrightarrow} \mathrm{UV} \qquad \text{S6-1}$$

where K is the equilibrium constant, and the value of K is set as 0.01 L/mol.

In a spectrum of a sample solution containing U and V, neither solvent nor V has any contribution in the spectral region investigated. U has a characteristic peak, and UV has a characteristic peak.

The characteristic peak of U can be described by a Gaussian function (Eq. S6-2).

$$f_U(x) = \varepsilon_U e^{-(ln2)\left[\frac{(x-X_U)^2}{W_U^2}\right]} = \varepsilon_U g_U(x) \qquad \text{S6-2}$$

where ε_U, X_U, and W_U, respectively are the molar absorptive, peak position, and half-width at the half-height of the characteristic peak of U.

The characteristic peak of UV can also be described by a Gaussian function (Eq. S6-3).

$$f_{UV}(x) = \varepsilon_{UV} e^{-(ln2)\left[\frac{(x-X_{UV})^2}{W_{UV}^2}\right]} = \varepsilon_{UV} g_{UV}(x) \quad \text{(S6-3)}$$

where ε_{UV}, X_{UV}, and W_{UV}, respectively are the molar absorptivity, peak position, and half-width at the half-height of the characteristic peak of UV.

The values of ε_U, X_U, W_U, ε_{UV}, X_{UV}, and W_{UV} are listed in **Table S6-1**.

Table S6-1 Peak parameters of U and UV in the model system 2

	Peak-position	Bandwidth	Absorbance
U	305.7	35	1.0
UV	304.1	36	1.0

To characterize the intermolecular interaction, five 1D spectra of the simulated solutions containing different amount of U and V are simulated. The initial concentration of U and V in the five simulated solutions are listed in **Table S6-2**. The simulated 1D spectrum are used to construct a 2D asynchronous spectrum.

Table S6-2 The initial concentrations of U and V

	C_U (mol/L)	C_V (mol/L)
1	0	0.1
2	0.35	0.1
3	0.37	0.1

4	0.39	0.1
5	0.38	0.1

Part 7 Detailed description on the analysis on the model system 2

As demonstrated previously, we assume the line $y = -x + \mathrm{b}$ is the mirror, where $\mathrm{b} \in [539.8, 679.8]$ (**Figure S7-1**). Then, we define two rectangular spectral regions (the two rectangular spectral regions are respectively denoted as Ω_1 and Ω_2). Ω_1 and Ω_2 are mirror images of each other with respect to the line $y = -x + \mathrm{b}$. The borders for Ω_1 are four lines that are defined by: $y = x$; $y = -x + \mathrm{b}$; $y = x + \alpha$; and $y = -x + (\mathrm{b} + \beta_1)$. The borders for Ω_2 are four lines that are defined by: $y = x$; $y = -x + \mathrm{b}$; $y = x + \alpha$; and $y = -x + (\mathrm{b} + \beta_2)$. The borders of the two rectangular regions are highlighted by dashed lines in **Figure S7-2**. In the present work, the values of α, β_1 and β_2 is set as 50, -50, and 50, respectively. To enhance the ability of the method to resist the interference of noise, both Ω_1 and Ω_2 is above the diagonal of the 2D asynchronous spectrum. The volumes of cross peaks in the two rectangular spectral regions (Ω_1 and Ω_2) are V_1 and V_2. In the corresponding $\Delta V \sim \mathrm{b}$ curve (**Figure S7-3**), the abscissa of the lowest point of the $\Delta V \sim \mathrm{b}$ curve is 587.

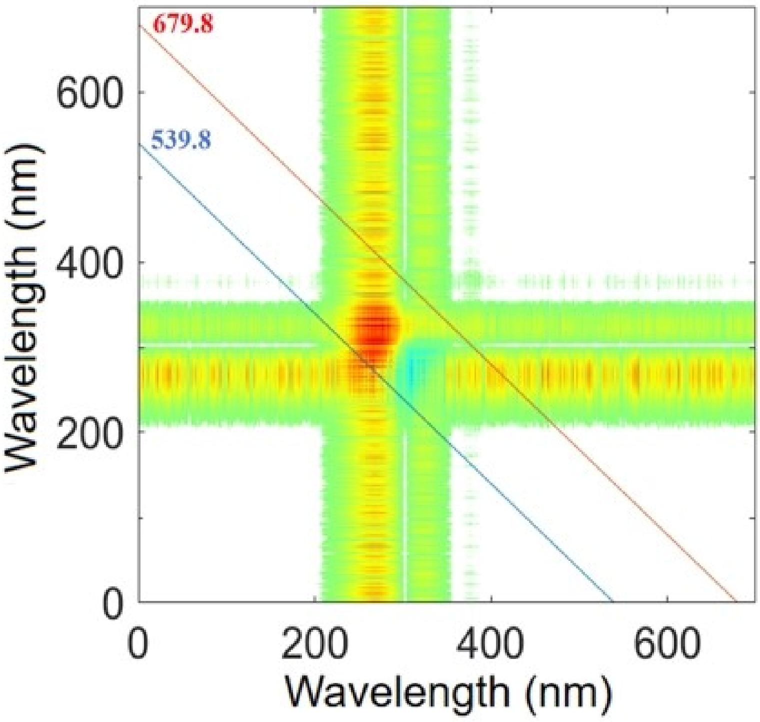

Figure S7-1. The b range in the model system 2.

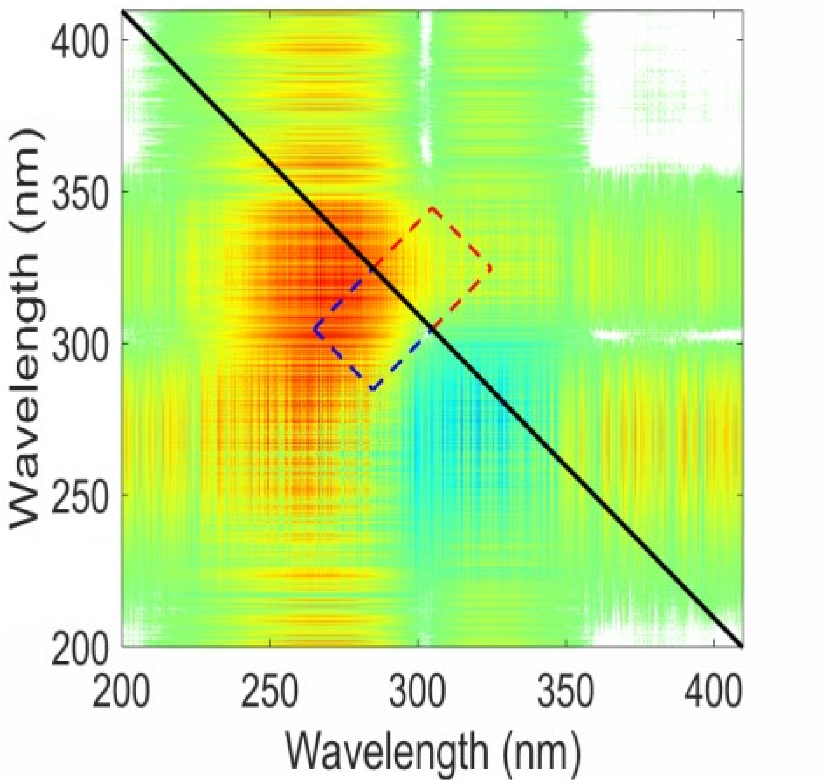

Figure S7-2. The borders of the two rectangular regions (Ω_1 and Ω_2) in the 2D asynchronous spectrum of the model system 2.

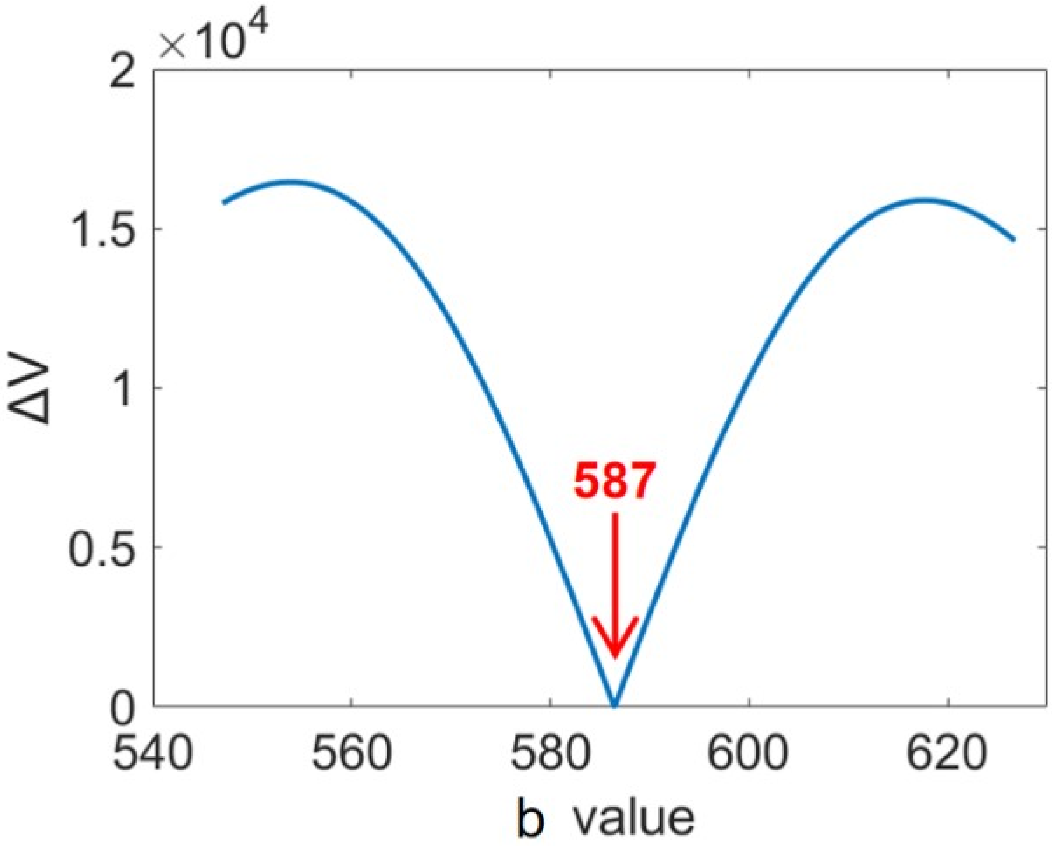

Figure S7-3. The corresponding ΔV ~ b curve of the model system 2.

Analysis of the model system 2 via the Kolmogorov-Smirnov two-sample test

15 pairs of small 2D spectral regions (${}^{i}\Omega_A$ and ${}^{i}\Omega_B$, where $i \in \{1, 2,\ldots,15\}$) are selected in a random manner. The borders for ${}^{i}\Omega_A$ are four lines that are defined by: $y = -x + {}^{i}b_1$, $y = -x + b_0$; $y = x + {}^{i}b_2$, and $y = x + {}^{i}b_3$. The borders for ${}^{i}\Omega_B$ are four lines that are defined by: $y = -x + (2b_0 - {}^{i}b_1)$, $y = -x + b_0$, $y = x + {}^{i}b_2$, and $y = x + {}^{i}b_3$. The values of ${}^{i}b_1$, ${}^{i}b_2$, and ${}^{i}b_3$ are generated within the following regions: ${}^{i}b_1 \in (615, 660)$; ${}^{i}b_2 \in (-90, -6)$; ${}^{i}b_3$

$\in (90, 6)$.

Table S7-1. The values of b_0, $^ib_1$, $^ib_2$, and $^ib_3$

i	b_0	$^ib_1$	$^ib_2$	$^ib_3$
1	560	614	-90	90
2	557	617	-84	84
3	554	620	-78	78
4	551	623	-72	72
5	548	626	-66	66
6	545	629	-60	60
7	542	632	-54	54
8	539	635	-48	48
9	536	638	-42	42
10	533	641	-36	36
11	530	644	-30	30
12	527	647	-24	24
13	524	650	-18	18
14	521	653	-12	12
15	518	656	-6	6

Table S7-2. The values of the P values in the 15 K-S tests of the model system 2 (The negative results are marked in red).

number	P value
1	0.6402
2	0.0000
3	0.0000
4	0.0000
5	0.8113
6	0.0000
7	0.0958
8	0.0000
9	0.9782
10	0.2565
11	0.7522
12	0.0000
13	0.9966
14	0.0051
15	0.6181

To prove that the cross peaks do not belong to the cross-peaks of type 3, the following analysis is performed.

We check whether the cross peaks shown in **Figure 3B** have a mirror symmetry with $x = X_U = 305.7$ nm, the K-S test is carried out.

The data of the first data set are selected randomly from the array of discrete data points within a rectangular region A ((255.7:305.7)⊗(200:400), the region is marked by a red rectangle in **Figure S7-4**. The size of the first data set is 1001. The data are $\{\Psi(x_A^1, y_A^1), \Psi(x_A^2, y_A^2), \ldots, \Psi(x_A^{1001}, y_A^{1001})\}$. The data of the second data set are selected from the array of the discrete data points within another rectangular region B ((305.7:355.7)⊗(200:400), the region is marked by a blue rectangle in **Figure S7-4**). The size of the second data set is also 1001.

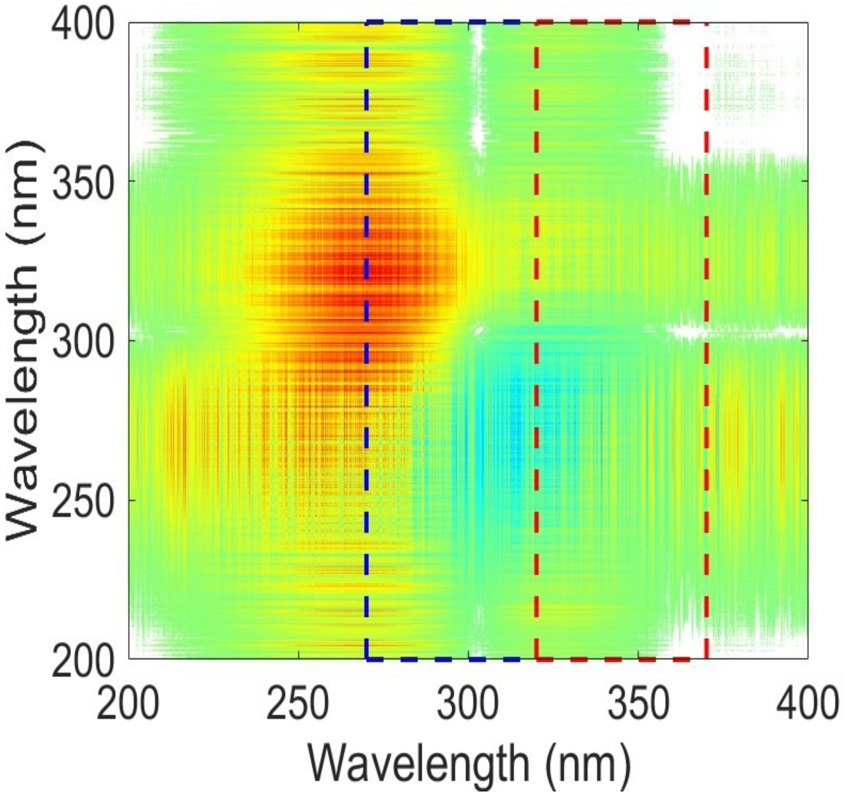

Figure S7-4 Two rectangular 2D spectral regions (region A and region B) in the 2D asynchronous spectrum, in which data-points are used in the K-

S test.

To check whether mirror symmetry occurs or not, it is wise that the data points in the first data set and those in the second data set are mirror images of one another with respect to the mirror (x = X_U = 305.7 nm). However, X_U is not exactly located at any discrete data point of the 1D spectrum. Moreover, X_U is not exactly located at any middle point between two adjacent discrete data points, either. Hence, the mirror images of the data points of the first data set cannot be within the array of discrete data points of the 2D asynchronous spectrum. Herein, the following rule is adopted in the selection of the data point of the second data set: For the i^{th} data point of the first data set, whose coordinates are (x_A^i, y_A^i), the coordinates of the corresponding point in the second data set is (x_B^i, y_A^i). In this case, x_B^i is the abscissa of a discrete data point in the 1D spectrum, which is the closest to the value of $2X_U$ - x_A^i (the mirror image of x_A^i with respect to x = X_U = 305.7 nm.

Subsequently, the two data sets are subjected to the K-S test. The calculation result shows that the value of P is 0.000. Therefore, we can reject H_0 and get a conclusion that there is no mirror symmetry with respect to x = X_U = 305.7 nm. Thus, the cross-peaks do not belong to the cross-peak of type 3.

Part 8 Description of the model system 3

In this model system, we try to characterize the intermolecular interaction between two solutes (S and R) dissolved in the same solutions.

Under the intermolecular interaction between S and R, part of S and part of R form a supramolecular aggregate (SR). The interconversion can be described by a reaction shown in Eq. S8-1.

$$S + R \overset{K}{\leftrightarrow} SR \qquad \text{S8-1}$$

where K is the equilibrium constant, and the value is set as 0.01 L/mol.

In a spectrum of a sample solution containing S and R, neither solvent nor R has any contribution in the spectral region investigated. S has a characteristic peak, and SR has a characteristic peak.

The characteristic peak of S can be described by a Gaussian function (Eq. S8-2).

$$f_S(x) = \varepsilon_S e^{-(ln2)\left[\frac{(x-X_S)^2}{W_S^2}\right]} = \varepsilon_S g_S(x) \qquad \text{S8-2}$$

where ε_S, X_S, and W_S, respectively are the molar absorptive, peak position, and half-width at the half-height of the characteristic peak of S.

The characteristic peak of SR can also be described by a Gaussian function (Eq. S8-3).

$$f_{SR}(x) = \varepsilon_{SR} e^{-(ln2)\left[\frac{(x-X_{SR})^2}{W_{SR}^2}\right]} = \varepsilon_{SR} g_{SR}(x) \qquad \text{(S8-3)}$$

where ε_{SR}, X_{SR}, and W_{SR}, respectively are the molar absorptivity, peak position, and half-width at the half-height of the characteristic peak of SR.

The values of ε_S, X_S, W_S, ε_{SR}, X_{SR}, and W_{SR} are listed in **Table S8-1**.

Table S8-1 Peak parameters of S and SR in the model system 3

	Peak-position	Bandwidth	Absorbance
S	305.7	35	1.0
SR	304.1	35.3	1.0

To characterize the intermolecular interaction, five 1D spectra of the simulated solutions containing different amount of S and R are generated. The initial concentration of S and R in the five simulated solutions are listed in **Table S8-2**. The simulated 1D spectrum are used to construct a 2D asynchronous spectrum.

Table S8-2 The initial concentrations of S and R

	C_S (mol/L)	C_R (mol/L)
1	0	0.1
2	0.35	0.1
3	0.37	0.1
4	0.39	0.1
5	0.38	0.1

Part 9. Detailed description on the analysis on the model system 3.

As demonstrated previously, we assume the line $y = -x + b$ is the mirror, where $b \in [539.8, 679.8]$ (**Figure S9-1**). Then, we define two rectangular spectral regions (the two rectangular spectral regions are respectively denoted as Ω_1 and Ω_2). Ω_1 and Ω_2 are mirror images of each other with respect to the line $y = -x + b$. The borders for Ω_1 are four lines that are defined by: $y = x$; $y = -x + b$； $y = x + \alpha$, and $y = -x + (b + \beta_1)$. The borders for Ω_2 are four lines that are defined by: $y = x$; $y = -x + b$； $y = x + \alpha$, and $y = -x + (b + \beta_2)$. The borders of the two rectangular regions are highlighted by dashed lines in (**Figure S9-2**. In the present work, the values of α, β_1 and β_2 is set as 50, -50, and 50, respectively. To enhance the ability of the method to resist the interference of noise, both Ω_1 and Ω_2 is above the diagonal of the 2D asynchronous spectrum. The volumes of cross peaks in the two rectangular spectral regions (Ω_1 and Ω_2) are V_1 and V_2. In the corresponding $\Delta V \sim b$ curve (**Figure S9-3**), the abscissa of the lowest point of the $\Delta V \sim b$ curve is 600.8.

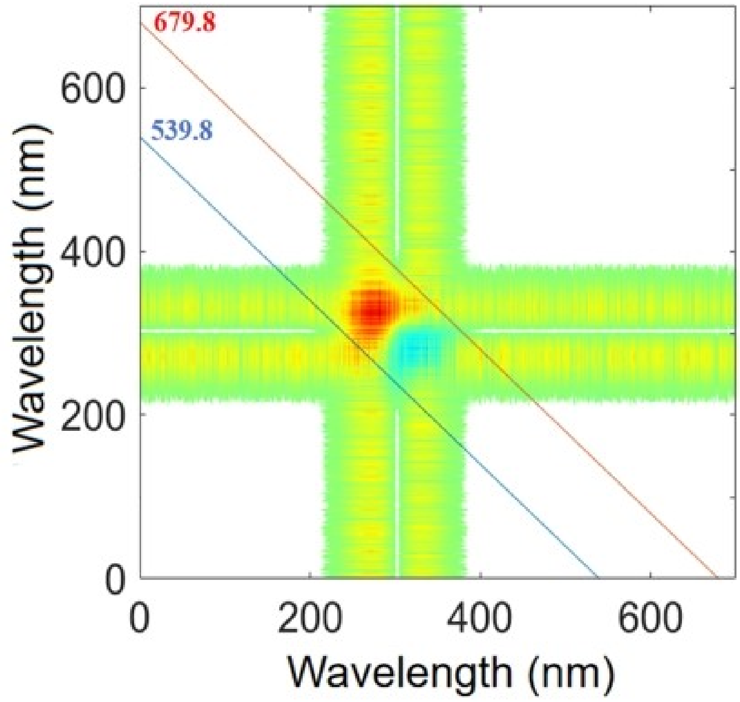

Figure S9-1. The possible range of b in the 2D asynchronous spectrum of the model system 3.

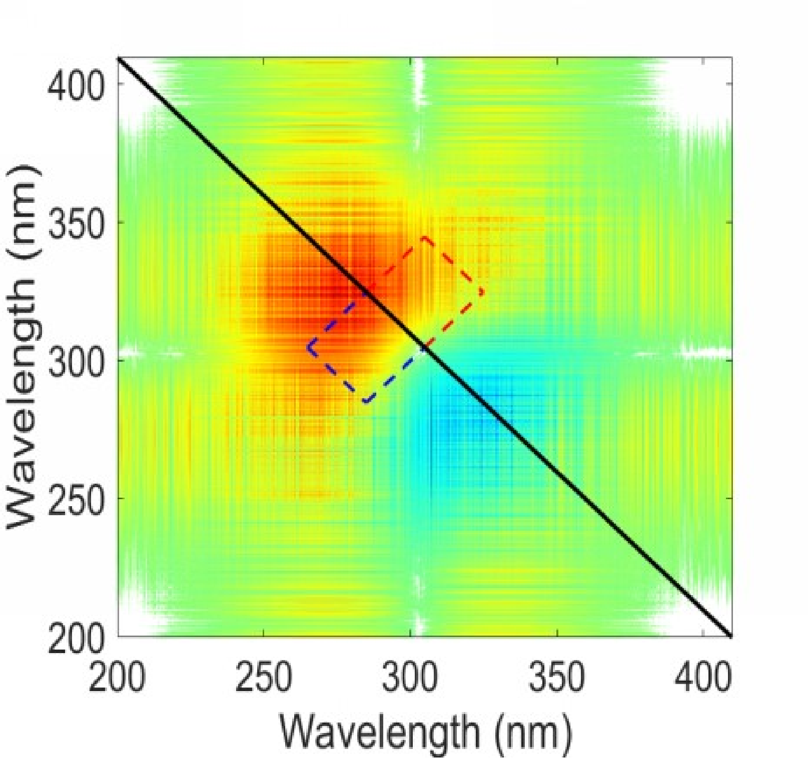

Figure S9-2. The borders of the two rectangular regions (Ω_1 and Ω_2) in the 2D asynchronous spectrum of the model system 3.

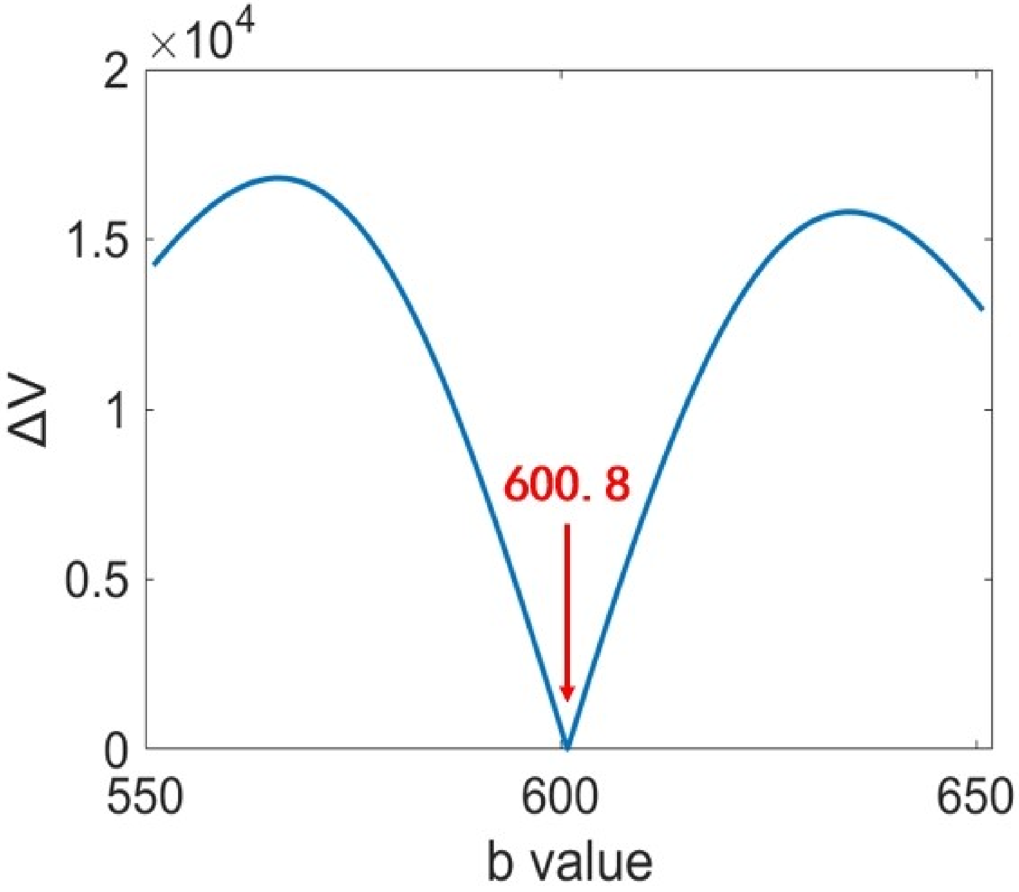

Figure S9-3. The corresponding ΔV ~ b curve of the model system 3.

Then, 15 pairs of small 2D spectral regions (${}^{\mathbf{i}}\Omega_A$ and ${}^{i}\Omega_B$, where $i \in \{1, 2, \ldots, 15\}$) are selected in a random manner. The borders for ${}^{\mathbf{i}}\Omega_A$ are four lines that are defined by: $y = -x + {}^{i}b_1$; $y = -x + b$, $y = x + {}^{i}b_2$, and $y = x + {}^{i}b_3$. The borders for ${}^{i}\Omega_B$ are four lines that are defined by: $y = -x + b$, $y = -x + 2b - {}^{i}b_1$, $y = x + {}^{i}b_2$, and $y = x + {}^{i}b_3$.

Then, the K-S test is performed to check whether the values of Ψ(x, y) in every pair of ${}^{\mathbf{i}}\Omega_A$ and ${}^{i}\Omega_B$ have the same distributions or not. The results of the K-S test shown in **Table S9-2** indicate that seven negative results of the K-S test are produced. Thus, we reject the hypothesis that the cross peaks do not have any mirror symmetry, and the cross peaks should belong to cross peaks of type 4. This result is in a good agreement with the preset peak parameters in **Table S8-1**.

Table S9-1. The volume of b_0, ${}^ib_1$, ${}^ib_2$ and ${}^ib_3$

i	b_0	${}^ib_1$	${}^ib_2$	${}^ib_3$
1	573.8	627.8	-90	90
2	570.8	630.8	-84	84
3	567.8	633.8	-78	78
4	564.8	636.8	-72	72
5	561.8	639.8	-66	66
6	558.8	642.8	-60	60
7	555.8	645.8	-54	54
8	552.8	648.8	-48	48
9	549.8	651.8	-42	42
10	546.8	654.8	-36	36
11	543.8	657.8	-30	30
12	540.8	660.8	-24	24
13	537.8	663.8	-18	18
14	534.8	666.8	-12	12
15	531.8	669.8	-6	6

Table S9-2. The P values of the 15 K-S tests in model system 3 (The negative results are marked in red).

number	P_i value
1	0.1264
2	0.4344
3	0.1216
4	0.0218
5	0.0050
6	0.5071
7	0.0622
8	0.1444
9	0.0057
10	0.0180
11	0.0809
12	0.7937
13	0.9931
14	0.0165
15	0.0182

Part 10 The detail description on the analysis of Benzene and Iodine system

Reagents

Chloroform (high-performance liquid chromatography (HPLC) grade), iodine, and benzene (AR grade) were purchased from Beijing Tong Guang Fine Chemicals Company.

Instrumentation

FTIR spectra of the samples were collected on a Thermo Fisher 6700 FTIR spectrometer. A BaF_2 cell with a specified path length (0.1 mm) was used in the experiment.

Table S10-1. The Initial Concentrations of Benzene and Iodine of the four Solutions

index	Benzene (mol/L)	Iodine ($\times 10^{-3}$mol/L)
1	0.225	0
2	0.451	1.42
3	0.563	2.54
4	0.789	4.07

Procedure to Generate 2D Asynchronous Spectra.

In the real-world example, four chloroform solutions containing different amounts of benzene and iodine were prepared. The initial concentrations of benzene and iodine are listed in **Table S10-1**. FTIR spectra of the four solutions were recorded at a resolution of 4 cm^{-1}, and 16 scans were co-added. Both 1D spectra obtained from the simulation on the model system and the experiment from the real-world example were used to generate 2D asynchronous spectra. The 2D asynchronous spectra were constructed based on the algorithm of Noda via scripts written in this lab using MATLAB software (MathWorks, Inc.). To enhance the intensities of cross-peaks, each 2D asynchronous spectrum was constructed without subtracting a reference spectrum.

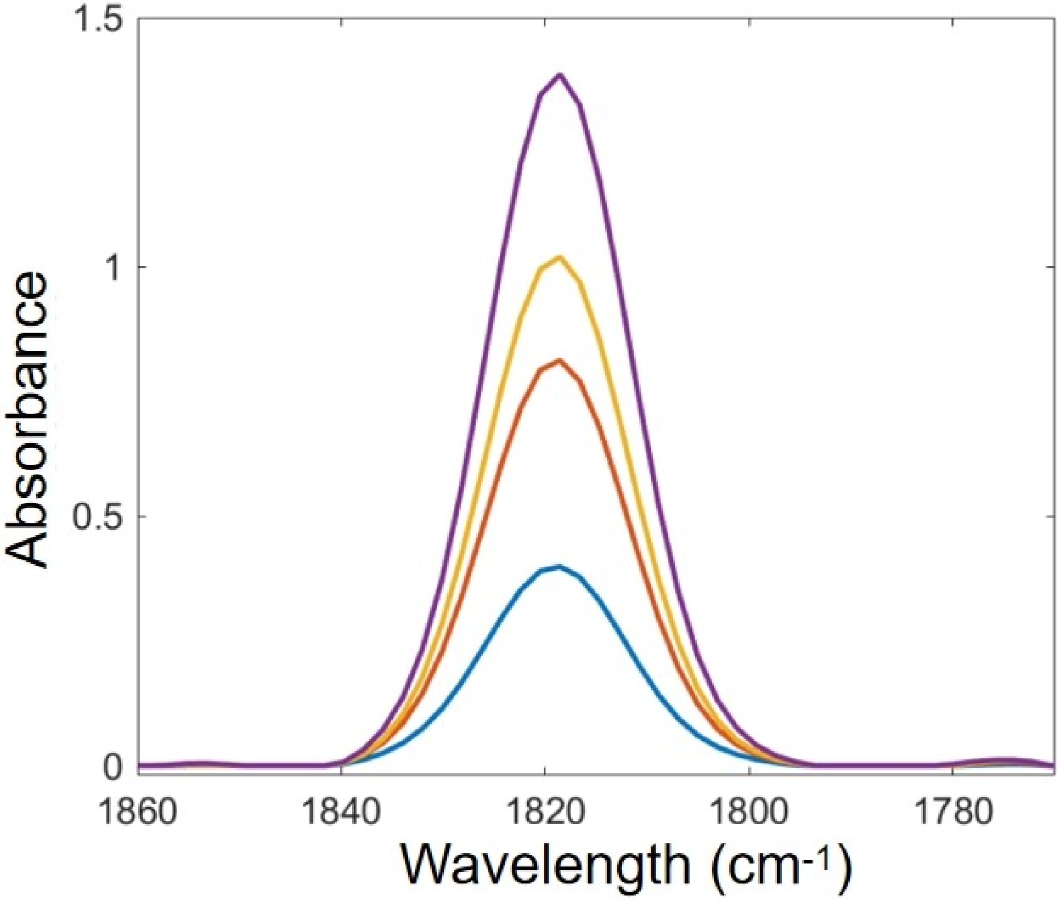

Figure S10-1. The four 1D spectra of Benzene and Iodine system

Adopted the KS-B method in the analysis of the cross peaks of the real-world system.

As demonstrated previously, we assume the line $y = -x + b$ is the mirror, where $b \in [3626, 3650]$ (**Figure S10-2**). Then, we define two rectangular spectral regions (the two rectangular spectral regions are respectively denoted as Ω_1 and Ω_2). Ω_1 and Ω_2 are mirror images of each other with respect to the line $y = -x + b$. The borders for Ω_1 are four lines that are defined by: $y = x$; $y = -x + b$; $y = x + \alpha$, and $y = -x + (b + \beta_1)$. The borders for Ω_2 are four lines that are defined by: $y = x$; $y = -x + b$; $y = x + \alpha$, and $y = -x + (b + \beta_2)$. The borders of the two rectangular regions are highlighted by dashed lines in **Figure S10-3**. In the present work, the values of α, β_1 and β_2 is set as 19, -19, and 19, respectively. To enhance the ability of the method to resist the interference of noise, both Ω_1 and Ω_2 is above the diagonal of the 2D asynchronous spectrum. The volumes of cross peaks in the two rectangular spectral regions (Ω_1 and Ω_2) are V_1 and V_2. In the corresponding $\Delta V \sim b$ curve (**Figure S10-4**), the abscissa of the lowest point of the $\Delta V \sim b$ curve is 3638.

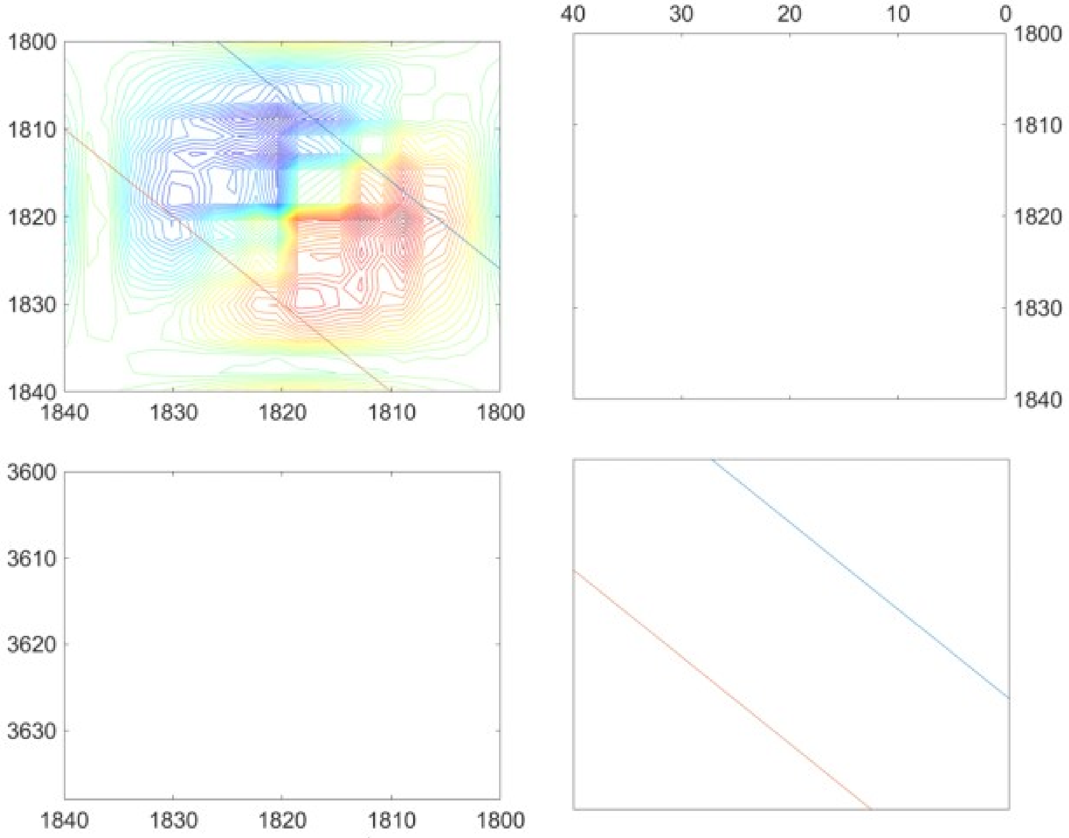

Figure S10-2. The possible range of b in the 2D asynchronous spectrum of the benzene/I_2 ystem

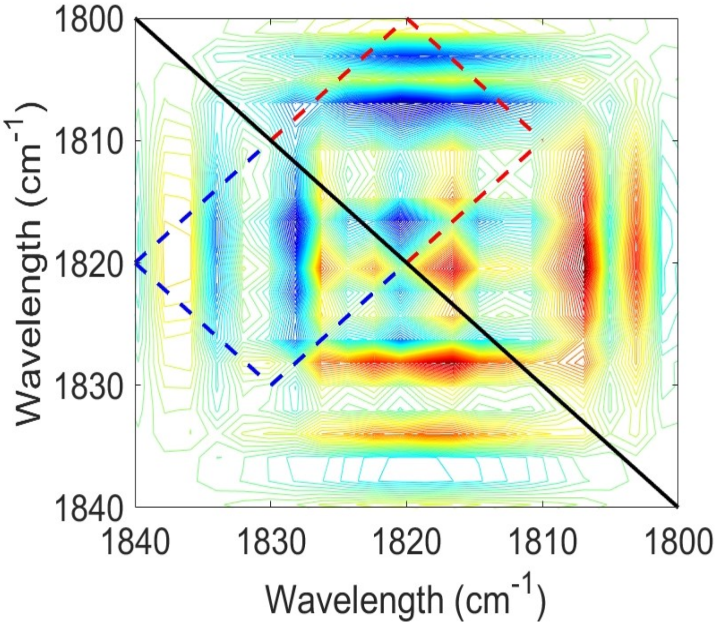

Figure S10-3. The borders of the two rectangular regions (Ω_1 and Ω_2) in the benzene/I_2 system.

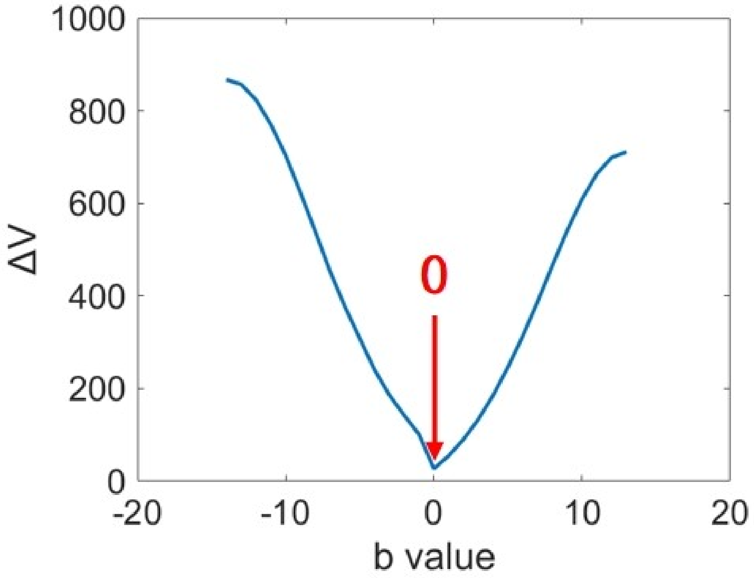

Figure S10-4. The corresponding ΔV ~ b curve of the noisy real-world system.

Then, 15 pairs of small 2D spectral regions (${}^{i}\Omega_A$ and ${}^{i}\Omega_B$, where $i \in \{1, 2, \ldots, 15\}$) are selected in a random manner. The borders for ${}^{i}\Omega_A$ are four lines that are defined by: $y = -x + {}^{i}b_1$, $y = -x + b_0$; $y = x + {}^{i}b_2$, and $y = x + {}^{i}b_3$. The borders for ${}^{i}\Omega_B$ are four lines that are defined by: $y = -x + (2b_0 - {}^{i}b_1)$, $y = -x + b_0$, $y = x + {}^{i}b_2$, and $y = x + {}^{i}b_3$. The values of ${}^{i}b_1$, ${}^{i}b_2$, ${}^{i}b_3$ and b_0 are listed in **Table S10-2**. For each i, ${}^{i}\Omega_A$ and ${}^{i}\Omega_B$ are mirror images to each other with respect to the line $y = -x+3638$.

Then, the K-S test is performed to check whether the values of $\Psi(x, y)$ in every pair of ${}^{i}\Omega_A$ and ${}^{i}\Omega_B$ have the same distributions or not. The results of the K-S test shown in **Table S10-3**. All the K-S tests produce positive results. Subsequently, $P_i(S_1)$ are calculated via Eq. 5 ~ Eq. 8. In the calculation, we hold a cautious attitude towards the assertion of a mirror symmetry occur in the cross peaks group under the investigation. Thus, $P_1(S_1)$ is set as a small value, i. e., $P_1(S_1) = 1.0\times10^{-9}$.

The resultant $P_{i(}S_1) \sim i$ curve depicted in **Figure 3B** turns out to be in a sigmoid shape. As i increases from 1 to 5, the value of $P_{i(}S_1)$ increases slightly. Then, a sharp increment in the values of $P_{i(}S_1)$ is observed when i changes from 6 to 9. Afterward, the value of $P_{i(}S_1)$ approaches 1.0 asymptotically as i is larger than 9. Since the ultimate $P_{i(}S_1)$ is near 1.0, demonstrating that the cross peaks possess mirror symmetry with respect to the line $y = -x+3628$.

Table S10-2. The values of b_0, ${}^{i}b_1$, ${}^{i}b_2$ and ${}^{i}b_3$

i	b_0	${}^{i}b_1$	${}^{i}b_2$	${}^{i}b_3$
1	3636	3640	1804	1834
2	3634	3642	1805	1835
3	3632	3644	1806	1836
4	3630	3646	1807	1837
5	3628	3648	1808	1838
6	3626	3650	1809	1839
7	3624	3652	1810	1840
8	3622	3654	1811	1841
9	3620	3656	1812	1842
10	3618	3658	1813	1843
11	3616	3660	1814	1844
12	3614	3662	1815	1845
13	3612	3664	1816	1846
14	3610	3666	1817	1847
15	3608	3668	1818	1848

Table S10-3. The value of P in the Benzene/I_2 system.

number	P value
1	0.4903
2	0.7237
3	0.9965
4	0.9027
5	0.9438
6	0.0656
7	0.9865
8	0.1625
9	0.9999
10	0.6585
11	0.9983
12	0.9999
13	0.2975
14	0.9921
15	0.1315